



Rapid autonomous analysis of HPGe spectra II: Uranium identification and characterization

Thomas B. Gosnell and James L. Wong

March 2014

Lawrence Livermore National Laboratory is operated by Lawrence Livermore National Security, LLC, for the U.S. Department of Energy, National Nuclear Security Administration under Contract DE-AC52-07NA27344.



Disclaimer

This document was prepared as an account of work sponsored by an agency of the United States government. Neither the United States government nor Lawrence Livermore National Security, LLC, nor any of their employees makes any warranty, expressed or implied, or assumes any legal liability or responsibility for the accuracy, completeness, or usefulness of any information, apparatus, product, or process disclosed, or represents that its use would not infringe privately owned rights. Reference herein to any specific commercial product, process, or service by trade name, trademark, manufacturer, or otherwise does not necessarily constitute or imply its endorsement, recommendation, or favoring by the United States government or Lawrence Livermore National Security, LLC. The views and opinions of authors expressed herein do not necessarily state or reflect those of the United States government or Lawrence Livermore National Security, LLC, and shall not be used for advertising or product endorsement purposes.

This work performed under the auspices of the U.S. Department of Energy by Lawrence Livermore National Laboratory under Contract DE-AC52-07NA27344.

**Rapid, autonomous analysis of HPGe gamma-ray spectra II:
Uranium identification and characterization**

Thomas B. Gosnell and James L. Wong

Table of Contents

| | |
|--|-----------|
| Rapid, autonomous analysis of HPGe gamma-ray spectra II: Uranium identification and characterization with RadID | 1 |
| Abstract | 4 |
| Introduction | 4 |
| Detecting the presence of uranium | 5 |
| Key full-energy peaks from uranium isotopes and collateral nuclides | 5 |
| Uranium-235—The only fissile primordial nuclide: | 6 |
| <i>Masking ²³⁵U</i> | 6 |
| Uranium-238—A fertile primordial nuclide: | 7 |
| <i>Identification of ²³⁸U in natural uranium</i> | 7 |
| Uranium-234—Naturally occurring, not primordial—another decay series nexus | 8 |
| Uranium-232—Possible HEU signature, parasitic impurity | 8 |
| Uranium-233—Looking to the future and the thorium fuel cycle..... | 8 |
| Uranium-236—Parent of ²³² U and ²²⁸ Th | 11 |
| Uranium-237— Fissions with fast neutrons, production of heat-source ²³⁸ Pu | 11 |
| Estimating uranium enrichment | 13 |
| Minimum enrichment estimation by peak-area ratio | 13 |
| Detecting HEU when no ²³⁸ U signal is manifest | 18 |
| Detecting shielded HEU | 18 |
| <i>Uranium-232: grasping at straws to detect shielded HEU</i> | 18 |
| <i>Distinguishing between ²³²U and ²³²Th</i> | 24 |
| Further distinguishing between natural U and processed U..... | 25 |
| The 609/1001 peak-area ratio..... | 25 |
| The 1001/766 peak-area ratio..... | 26 |
| Conclusion | 27 |
| Acknowledgements..... | 27 |
| Appendix A: The uranium decay series..... | 28 |
| Appendix B: The thorium decay series..... | 29 |
| Thorium-228: Nexus nuclide—a ubiquitous and ambiguous signature | 29 |
| Appendix C: About uranium | 31 |
| Natural uranium | 31 |
| Uranium ore | 31 |
| Enriched uranium | 31 |
| Fluorine in uranium—Uranium hexafluoride and uranyl fluoride | 31 |
| Reprocessed uranium | 33 |

The uranium contribution to background spectra 34
More observations about background interference in field measurements..... 36
References 37

Abstract

RadID is a gamma-ray spectrum analysis program originally written to assist in the detection of the illicit movement of nuclear material. It is specific to the rapid analysis of HPGe gamma-ray data to reveal the radionuclide signatures of interest that may be present in the spectra. It is an autonomous, rule-based heuristic system that can identify well over 200 radioactive sources in about one second. *RadID* does not require knowledge of the detector efficiency, the source-to-detector distance, or the geometry of the inspected radiation source—including any shielding. In this second of a three-document series we discuss how *RadID* detects the presence of uranium isotopes and determines a number of its characteristics, most notably: natural or processed material and enrichment estimates.

Introduction

Every gamma-ray spectrum tells a story and, like a book, it can be read if you understand the language. A book in good condition with crisp print can be easily read. A book in poor condition, such as a tattered ancient biblical scroll with voids in the document, can only be read with imprecision. Similarly, a gamma-ray spectrum acquired in the field for a brief period of time and smeared by a detector with poor energy resolution is likely to be read with similar imprecision, sometimes resulting in nuclide misidentification [1].

Some gamma-ray spectra are collected by in the field, under suboptimal conditions, for short periods of time, and can result in sparse data that cannot reveal the finest details. Nevertheless, the superior energy resolution of HPGe spectra provides considerably greater information content than is found in commonly employed scintillation detectors, such as NaI(Tl) [1]. For this reason, HPGe excels in the analysis of complex spectra from sources of mixed radionuclides [2] such as uranium. This is true even for spectra from high-resolution detectors where only the most intense peaks can regularly be observed with confidence.

RadID is a modified version of an earlier code written for nuclear emergency response. For this rapid nuclide identification is of the essence. Data acquisition times are short, in the neighborhood of 600 seconds and almost always done out of doors. Program execution time also needs to be rapid. For this reason, *RadID* is based on an expert system [3,4]. Once feature extraction is performed, the system traverses a decision tree with a Boolean result at each branch that is accomplished in about one second. For this reason, *RadID*'s personality is a strong reminder of its original *raison d'être*.

Detecting the presence of uranium

Key full-energy peaks from uranium isotopes and collateral nuclides

There are many isotopes of uranium. In this section we discuss those that occur in nature or are the result of reprocessing uranium. The radiation signatures of uranium vary from its natural states to its many processed forms. While there are hundreds of gamma rays emitted by these nuclides and their decay daughters, the vast majority of these emissions are too weak to be reliably observed with field measurements of typically short duration. For rapid identification of uranium from sparse gamma-ray spectra, of necessity, we need to be concerned with the most intense gamma rays associated with their decay. These are shown in Table 1 with their energies and emission intensities in percent, $I\gamma(\%)$, along with others that are mentioned in this paper.

Table 1. Key peaks and emission intensities from uranium isotopes and collateral nuclides [5]

| Nuclide | Daughters | Energy (keV) | $I\gamma(\%)$ | Nuclide | Daughters | Energy (keV) | $I\gamma(\%)$ | | |
|------------------|--------------------|-------------------|---------------|---------------------------------------|---------------------------------------|-------------------|---------------|-----------|------------|
| U | U Ka1 X-ray | 98.44 | (100 rel.) | ¹⁹ F | Stable no γ | | | | |
| | U Kb1' X-ray | 111. | (38 rel.) | | ¹⁹ F(a,n) ²² Na | 1274.53 | | | |
| ²³² U | | 57.77 | 0.1999 | ¹⁹ F(a,p) ²² Ne | 1274.53 | | | | |
| | | 129.06 | 0.0682 | Pb | Pb Ka1 X-ray | 74.97 | (100 rel.) | | |
| | | 270.24 | 0.00316 | | Pb Ka2' X-ray | 84.8 | (35 rel.) | | |
| | ²⁰⁸ Tl | | 328.00 | 0.00283 | ²¹⁴ Bi | | 609.31 | 46.1 | |
| | | 583.19 | 84.5 | | | 768.36 | 4.94 | | |
| | | 2614.53 | 99. | ²²⁶ Ra | | 186.21 | 3.59 | | |
| ²³³ U | | 317.16 | 0.00776 | | ²¹⁴ Pb | | 242.00 | 7.43 | |
| | | 320.54 | 0.00290 | | | | 295.22 | 19.3 | |
| | | 323.42 | 0.00077 | | | 351.93 | 37.6 | | |
| ²³⁴ U | | 120.9 | 0.0342 | ²³³⁷ Np | Np Ka1 X-ray | 101.07 | (100 rel.) | | |
| ²³⁵ U | | 143.76 | 10.96 | | Np Kb1' X-ray | 104. | (39 rel.) | | |
| | | 163.36 | 5.08 | | ²³³ Pa | 300.34 | 6.62 | | |
| | | 185.70 | 57.2 | | | 312.17 | 38.6 | | |
| | | 205.31 | 5.01 | | 340.81 | 4.47 | | | |
| ²³⁸ U | | Various | Weak | ²²⁸ Ac | | 911.20 | 25.8 | | |
| | ^{234m} Pa | | 766.38 | 0.294 | ²²⁸ Th | | Few | Weak | |
| | | | 1001.03 | 0.837 | | ²⁰⁸ Tl | 583.19 | 84.5 | |
| | | | 186.21 | 3.59 | | 2614.53 | 99. | | |
| | ²²⁶ Ra | | 186.21 | 3.59 | ²¹² Pb | | 238.63 | 43.3 | |
| | | ²¹⁴ Pb | | 242.00 | | 7.43 | Bi Ka1 X-ray | 77.11 | (100 rel.) |
| | | | | 295.22 | | 19.3 | Bi Ka2' X-ray | 87.2 | (36 rel.) |
| | | 351.87 | 37.6 | ²³⁸ Pu | | 766.38 | 0.000022 | | |
| | ²¹⁴ Bi | | 609.31 | | 46.1 | | 1001.03 | 0.0000010 | |
| | | | 768.36 | | 4.94 | ²³⁹ Pu | | 375.04 | 0.001554 |
| | | | | | 413.71 | | 0.001416 | | |

Uranium-235—The only fissile primordial nuclide:

Uranium-235 does not usually display a usable gamma-ray signature in background radiation because it is masked by ^{226}Ra . The distinguishing radiation signature of ^{226}Ra is the picket-fence-like structure of four peaks ranging from 186- to 352-keV shown in the uranium ore spectrum shown in Fig. C-3, in Appendix C. From Table 1 we see that the most intense gamma ray from ^{235}U occurs at 185.70-keV ^{226}Ra emits a gamma ray at 186.21-keV. “These peaks are so close together that deconvolution in environmental spectra is unlikely to give results that one can have confidence in [6].” Unshielded or lightly shielded processed ^{235}U is easily detected by the presence of the four ^{235}U low-energy gamma rays at 143-, 163-, 186-, and 205-keV and the absence of strong peaks from ^{214}Pb as shown in Fig. 1.

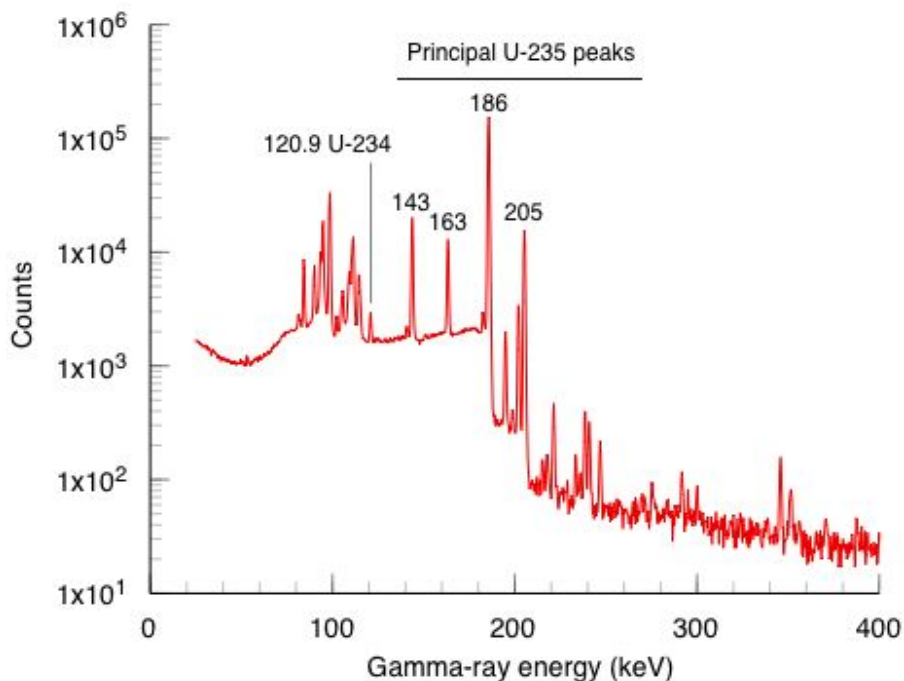


Fig. 1. Low-energy portion of a gamma-ray spectrum of uranium, enriched to 93% ^{235}U , showing the key peaks used for identification of the presence of ^{235}U and the 120.90-keV peak from ^{234}U decay.

Masking ^{235}U

If the four characteristic ^{235}U gamma peaks are manifest, we can have high confidence in the identification of ^{235}U . However, weak emissions, shielding, or downscatter from higher energy peaks can obscure the peaks at 143-, 163-, and 205-keV, such that only the 185.7-keV peak remains manifest. Several radionuclides of interest in *RadID* have strong gamma lines near 185.7-keV and can mask the presence of HEU in situations where the ^{238}U signature is too weak to be manifest as well. These nuclides are medical ^{67}Cu (184.58-keV), medical ^{67}Ga (184.58-keV, same gamma ray as ^{67}Cu), check source $^{166\text{m}}\text{Ho}$ (184.41-keV), and naturally occurring ^{226}Ra (186.21). The *RadID* rules include a section that steps through each of these nuclides and provides methods that undertake detecting such masking.

Uranium-238—A fertile primordial nuclide:

Direct radiations from long-lived ^{238}U are too weak or too low in energy to be useful for field identification. This is also true of its daughter ^{234}Th . From Fig. A-1, in Appendix A, we observe that ^{234}Th has a half-life of 24.1 days. Within five ^{234}Th half-lives, or less than 5 months, secular equilibrium of ^{234}Th will be within a few percent of establishment. $^{234\text{m}}\text{Pa}$ with its half-life of 1.17m will have been in equilibrium with ^{234}Th in minutes. The distant daughters of ^{238}U , particularly ^{226}Ra , ^{214}Pb , and ^{214}Bi account for a majority of the peaks manifest in the spectrum of uranium ore. Thorium-234 in turn largely decays to the metastable state of its daughter $^{234\text{m}}\text{Pa}$ that then largely beta decays directly to excited states of ^{234}U . These states emit highly penetrating gamma-ray emissions at 766.41- and 1001.03-keV. The presence of ^{238}U can be provisionally inferred from the presence of these two gamma rays.

Identification of ^{238}U in natural uranium

In natural uranium it is tempting to simply identify the presence of ^{238}U solely from the 766.41 and 1001.03-keV peaks, however there is interference from an unresolved ^{214}Bi peak from natural uranium at 768.38-keV (Fig. 2). We found that, for detection of ^{238}U , integrating the doublet, rather than resolving it, is desirable. Furthermore, the presence of uranium ore, identified from the presence of manifest ^{226}Ra , and the 1001.03-keV $^{234\text{m}}\text{Pa}$ gamma ray indicate that ^{238}U is present. In chemically processed uranium, the processing removes the ^{238}U daughters, except for ^{234}U and ingrowth of ^{226}Ra and its ^{214}Bi daughter gamma ray at 768.36-keV is too slow to be competitive with the ^{238}U 766.41-keV peak in a human lifetime. So tentative identification of ^{238}U is possible with the presence of the 766.38 and 1001.03-keV gamma rays. Their presence is necessary but not sufficient to avoid misidentification as ^{238}Pu .

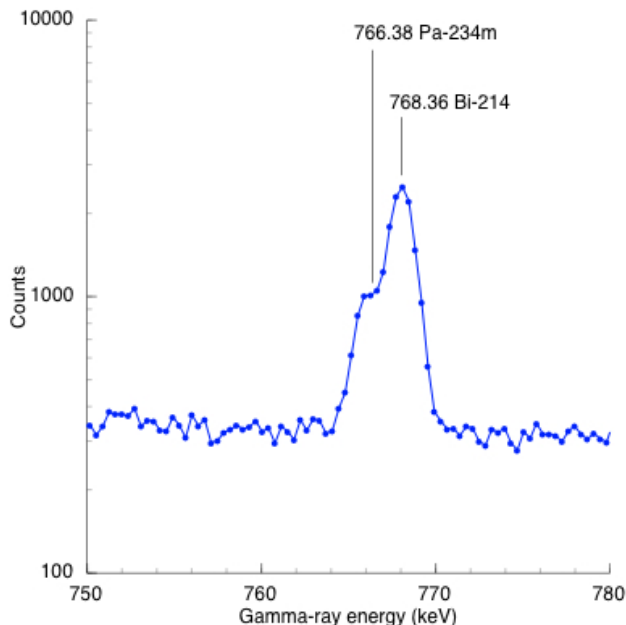


Fig. 2. The doublet formed by the 766.41 $^{234\text{m}}\text{Pa}$ peak and the 768.36-keV peak from ^{214}Bi in the uranium ore spectrum shown in Fig. C-2, in Appendix C.

Uranium-234—Naturally occurring, not primordial—another decay series nexus

Uranium-234 is naturally occurring but not primordial because its half-life is only 245,500 years. Its existence is the result of the decay of primordial ^{238}U and is its great-granddaughter. It makes up only 0.0055% of natural uranium. The importance of ^{234}U for uranium identification is that its excited states yield the dominant gamma rays that indicate the presence of ^{238}U . These same gamma rays, but with extremely low emission intensities and different *relative* intensities, are also the dominant signature of substantial quantities of ^{238}Pu .

Enriched uranium contains more ^{234}U than natural uranium as a byproduct of the uranium enrichment that concentrates lighter isotopes even more strongly than it does ^{235}U [7]. While ^{234}U is not fissile it is fertile and absorbs slow neutrons in a nuclear reactor to become fissile ^{235}U . This may be undesirable in some reactors as it changes the reactivity of the uranium [8].

The presence of ^{234}U in the gamma-ray spectrum of HEU can be observed although its gamma-ray emissions are quite weak. The two strongest are 53.20-keV at 0.123% emission intensity and 120.90-keV at 0.0342%. The low-energy region of the gamma-ray spectrum of WGU is shown in Fig. 9. The detector efficiency is degraded at 53-keV but an apparent tiny visible peak at about 53-keV might be from ^{234}U . The detector is far more efficient at 121-keV and a small peak is manifest between the “forest” of low-energy gamma rays and U K-series X-rays below about 115-keV and the 143-keV ^{235}U gamma ray.

Uranium-232—Possible HEU signature, parasitic impurity

With only a 69-year half-life, ^{232}U does not occur in nature but is introduced as a result of reactor irradiation of uranium. In the 1960's, uranium that had previously been irradiated in reactors was introduced into U.S. gaseous diffusion plants to be re-enriched. Consequently, trace quantities of ^{232}U were entrained in the gaseous diffusion cascades where they remain today and became a minor contaminant in new feedstock as it was introduced to the cascade. During enrichment it is preferentially swept into the light isotope fraction that becomes HEU. Its presence as a possible indicator of shielded HEU is discussed in a following section.

Uranium-232 is found in reprocessed uranium. During its irradiation in a reactor, uranium is profoundly modified. It contains all the isotopes of uranium between ^{232}U and ^{238}U except ^{237}U , which is rapidly transformed into ^{237}Np . **Its**

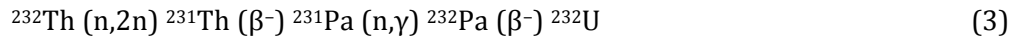
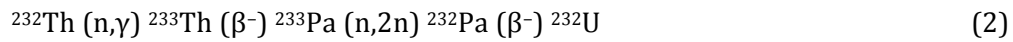
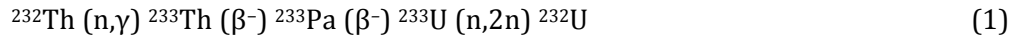
Uranium-232 is **also** a parasitic impurity formed in the production of fissile ^{233}U . Its importance is discussed in the following description of ^{233}U .

Uranium-233—Looking to the future and the thorium fuel cycle

Uranium-233 is a fissile uranium isotope with a half-life of 159.2 thousand years that does not occur in the earth's crust. It is bred from ^{232}Th to become part of a thorium fuel cycle. **Because ^{233}U is fissile, there have been concerns that it could be used in nuclear weapons. ^{233}U has also been considered as a reactor fuel but was never used commercially for this purpose. Because it is fissile, it was investigated in the U. S. in the past for use in nuclear**

~~weapons and as a reactor fuel. However, until recently, it was never used for these purposes [37].~~ This is because the intense gamma radiation from the decay daughters of parasitic ^{232}U , a byproduct of ^{233}U production, makes the ^{233}U hazardous to handle.

Production of ^{233}U via neutron irradiation of ^{232}Th produces small amounts of ^{232}U as an impurity, because of (n,2n) reactions on ^{233}U itself, or on ^{233}Pa [88, 99]:



The decay products of parasitic ^{232}U enter the thorium decay series and, because of its high specific activity relative to other present uranium isotopes, quickly yield a strong ^{228}Th signature [Fig. B-2, appendix B]. For this reason ^{232}U has been cited as an obstacle to nuclear proliferation by using ^{233}U as the fissile material [1040]. This is because it makes manual spent fuel handling in a glove box with only light shielding (as commonly done with plutonium) too hazardous, (except possibly in a short period immediately following chemical purification of the uranium). Instead it will require using costly remote manipulation.

~~In addition, the decay heat released can cause problems in weapons design, for example, thermal degradation of high explosives [41].~~

Nevertheless, international interest in thorium energy has renewed [112]. Moreover, for over 50 years India has invested in the long-term development of a thorium fuel cycle. India's vast population and widespread poverty places it in great need of increased energy production to improve quality of life. India's coal and uranium reserves are limited. However, India's reserve in thorium is estimated at 300,000 metric tons. With the country's great need for energy and its vast thorium reserves, in the 1950's Indian physicist Homi Jehangir Bhabha proposed a three-stage program to bootstrap its limited nuclear resources into a viable thorium-based nuclear energy program [120]. This thorium fuel cycle is expected to lead to the use of thorium-based reactors to meet 30% of its electricity demands by 2050 [133]. The Indian plan has entered its third stage and a thorium fuel cycle Advanced Heavy Water Reactor (AHWR) with mixed oxide fuel (Th-LEU) is planned for operation before the end of this decade.

Anticipating the possible future appearance of illicit ^{233}U "in the wild," it is prudent to examine its likely gamma-ray signature. With a uranium isotopic vector at reactor discharge, we can model its likely gamma-ray spectrum and study the effect of ^{228}Th ingrowth on the spectral structure as a function of time. This structure will depend on the nature of the reactor fuel and its burnup. We can use the projected AHWR uranium isotopic input and output vectors [144], shown in Table 2, to illustrate the rapidity of ^{228}Th ingrowth.

Table 2. Uranium isotopic vectors for initial and discharged AWHR fuel

| Fuel burn-up | ^{232}U % | ^{233}U % | ^{234}U % | ^{235}U % | ^{236}U % | ^{237}U % | ^{238}U % |
|--------------------------|--------------------|--------------------|--------------------|--------------------|--------------------|--------------------|--------------------|
| Initial | 0.0 | 0.0 | 0.0 | 19.75 | 0.0 | 0.0 | 80.25 |
| Discharge (64 GWd/Te) | 0.02 | 6.51 | 1.24 | 1.62 | 3.26 | 0.00 | 87.35 |

We modeled expected spectra from a 20% HPGe detector, as a function of time following discharge, for 1000-s counts at 1-meter from a 5-kg sphere, formed from this output vector. This is shown in Fig. 3.

After 1-day, the ^{228}Th signature is already strongly present but structure from other nuclides, including direct decay gamma rays from ^{232}U and ^{233}U below 400 keV, is also manifest. After 1-week, the ^{228}Th structure is largely dominant. After 1 month and certainly 1-year, the ^{228}Th structure almost completely masks the presence of other nuclides.

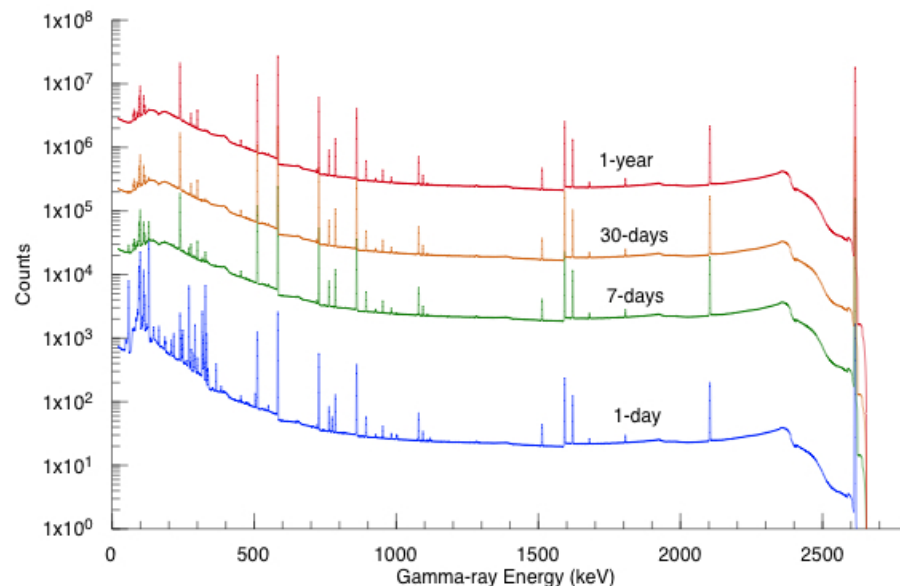


Fig. 3. Simulated 1000-s gamma-ray spectra from 5 kg of chemically separated uranium from discharged AWHR fuel containing 0.02% of parasitic ^{232}U . We follow the evolution of the spectral structure as a function of time (1-d, 7-d, 30-d, and 1-year) following discharge. At 1-day, the bulk of the structure occurs below 400 keV. This structure becomes increasingly masked with the rapid ingrowth of a ^{228}Th spectrum with only uranium f K-series X-rays that reveal that these spectra are from a uranium source.

Comparing the region below 300 keV in the 1-y AWHR spectrum with the point source ^{228}Th spectrum in Fig. B-2, self-attenuation is apparent and greater annihilation is notable in the AWHR spectrum from a 5-kg uranium sphere. Where the spectral structure differs between the uranium and thorium sources is below 120-keV and shown in Fig. 4. In the ^{228}Th spectrum, we see strong K X-ray structure between 70- and 90-keV, largely from Bi and Pb X-rays. These X-rays survive in the AWHR discharge spectrum as ^{228}Th is the daughter of

^{232}U . However, in the AHWR discharge spectrum we observe the strong presence of uranium K X-rays from decay of $^{234\text{m}}\text{Pa}$ between 92- and 111-keV that grow in concert with the increasing ^{228}Th spectrum that stimulates the uranium in the 5 kg sphere. These characteristic uranium X-rays can be expected to be of little utility as a surrogate for ^{233}U detection because the source would likely be shielded for personnel safety.

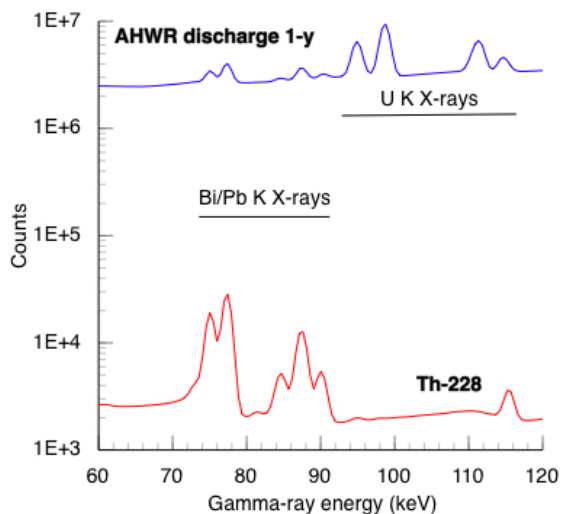


Fig. 4. The spectrum from AHWR discharge exhibits a strong ^{228}Th signature but differs from the ^{28}Th signature below 120 keV with the presence of a pronounced uranium K X-ray structure.

Uranium-236—Parent of ^{232}U and ^{228}Th

Uranium-236 is neither fissile, nor very good fertile material but is generally considered a nuisance and long-lived radioactive waste. It is found in spent nuclear fuel and in reprocessed uranium made from spent nuclear fuel [155].

Uranium-236 is the parent of ^{232}U that decays to ^{228}Th in the thorium decay series. That produces a ubiquitous, and therefore ambiguous, radiation signature (Appendix B).

The use of uranium re-enriched from spent reactor fuel (RU) in a closed fuel cycle was studied during the short-lived U. S. participation in the Global Nuclear Energy Partnership (GNEP) [166] between 2006 and 2009 [177]. The small amounts of $2.342\text{E}7\text{-y } ^{236}\text{U}$ in RU would act as a poison and reduce the reactivity of the re-enriched reactor fuel [188, 199].

Uranium-237— Fissions with fast neutrons, production of heat-source ^{238}Pu

Uranium-237 is present in reprocessed uranium. When separated from the reprocessed uranium, its 6.75-d half-life causes it to decay rapidly to $2.144\text{e}6\text{-y } ^{237}\text{Np}$. ^{237}Np is used in the production of heat-source plutonium, dominated by ^{238}Pu .

^{237}Np is a nuclide of considerable interest because it is also capable of sustaining a chain reaction with fast neutrons. Commercial nuclear reactors annually create tons of neptunium mixed in with other nuclear waste. Since 1999, the International Atomic Energy Agency in Vienna has urged monitoring of neptunium. However, according to the agency, the risk of

anyone making neptunium bombs from such highly radioactive waste is low because it would be so difficult to extract the isotope [20].

Neptunium-237 is the progenitor of yet another decay series, the neptunium series. It undergoes alpha decay to ^{233}Pa . The gamma rays associated with this decay are too low in energy and too feeble to be of use for rapid ^{237}Np detection. However, its daughter, ^{233}Pa , with a 225.97-d half-life grows rapidly into secular equilibrium and can act as a detection surrogate. It undergoes β^- decay with accompanying emission of relatively strong gamma rays at 300.34-, 312.17-, and 340.81-keV. The identity of neptunium would likely not be lost in the decay of a significant mass of ^{237}Np with the production of Np K-series fluorescent X-rays.

Estimating uranium enrichment

Minimum enrichment estimation by peak-area ratio

In principle, uranium enrichment can be determined by measuring the ratio of counts in the 185.71-keV ^{235}U peak and the 1001.03-keV peak from the ^{234}Pa granddaughter of ^{238}U . In the uranium spectra shown in Fig. 5, the increase in the height of the 186-keV ^{235}U peak relative to the 1001-keV ^{238}U peak as a function of increasing enrichment is readily apparent.

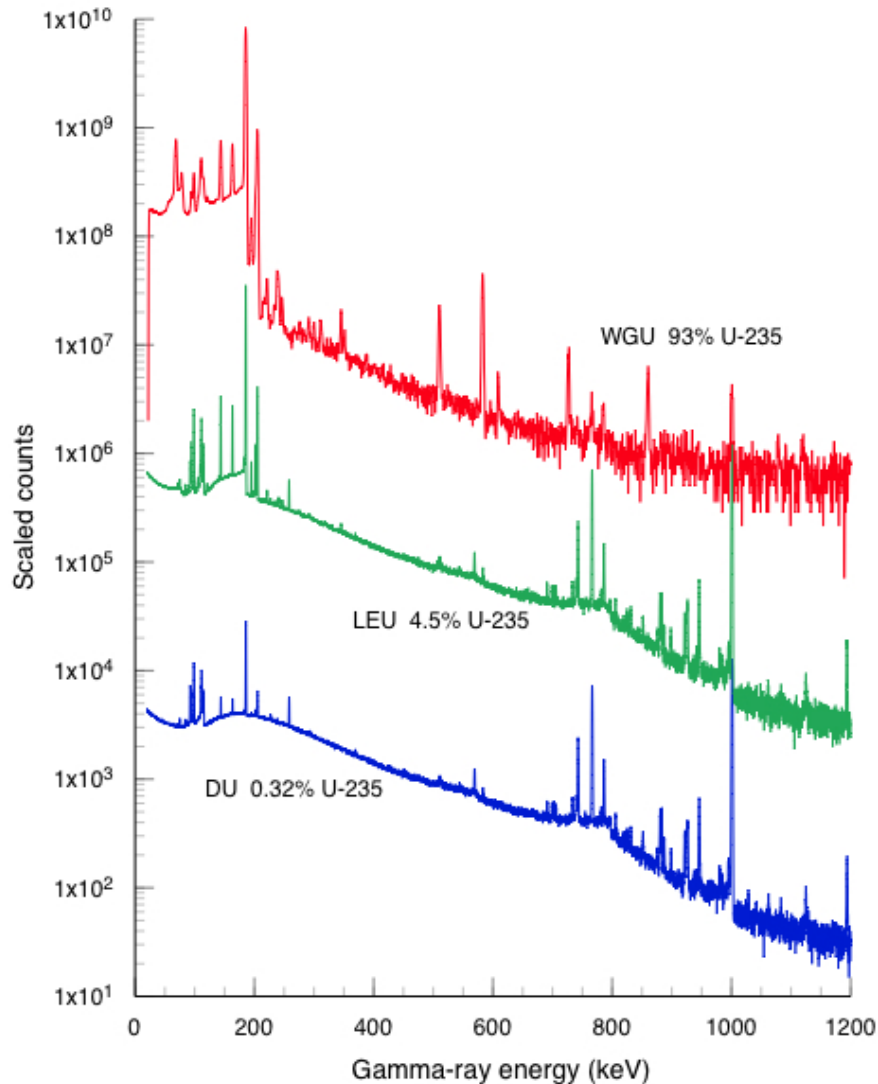


Fig. 5. Uranium spectra from standards of three different enrichments. The top two spectra have been scaled to separate them for presentation. All three were acquired with HPGc detectors of 20% relative efficiency at a source distance of 100 cm. The lower two spectra were counted for 7000 seconds. The upper spectrum, a weaker source, was counted for only 900 seconds.

In the early 1970's an effort was made to apply this ratio to obtain high precision, high accuracy results. It was not found to be fruitful for this purpose because certain required information was unavailable for field use [21]. It has also been observed that although the 186- and 1001-keV peaks are easy to measure, it is difficult, because of the large difference in their energies, to determine the relative efficiencies with which they are detected [54-22].

Furthermore, if there is material intervening between the uranium and the detector, the 186 keV peak will be preferentially attenuated relative to the 1001 keV peak, resulting in an enrichment estimate that is too low, a lower limit or minimum estimate.

Our goal is considerably less ambitious in terms of precision and accuracy. We do, however, wish to make at least a rough estimate of minimum enrichment grade. The task is challenging: to be able to make this enrichment estimate with an automated analysis tool that doesn't require knowledge of the nature of the source, the source-to-detector measurement distance, or the efficiency of the detector. To do so, we have resorted to some sweeping assumptions that have led to solutions that are imprecise but we nevertheless find useful.

If N_x is the number of atoms of isotope x in a gram of uranium, then the number of counts from a particular gamma ray $C_{\gamma x}$ from that isotope observed by a detector at a distance r in a counting interval t_x is

$$C_{\gamma x} = N_x \lambda_x I_{\gamma x} t_x \epsilon_{\gamma x} \alpha_x \beta_x \quad (4)$$

where λ_x is the isotope decay constant, $I_{\gamma x}$ is the emission probability per decay of a particular gamma ray γ , $\epsilon_{\gamma r}$ is the detection efficiency for the gamma ray at distance r , α_x is an external absorber correction, and β_x is a correction for sample self-absorption.

We note that the first three terms of Eq. 4 compute the specific emission rate $S_{\gamma x}$ ($\gamma/s/g$) of the gamma ray. If we now measure a uranium item and take the ratio of the counts from the 185.7-keV gamma ray from ^{235}U (C_{235}) and the counts from to 1001.03-keV gamma ray from ^{238}U (C_{238}), we arrive at Eq. 5.

$$\frac{C_{235}}{C_{238}} = \frac{S_{235}}{S_{238}} \cdot \frac{\epsilon_{235}}{\epsilon_{238}} \cdot \frac{\alpha_{235}}{\alpha_{238}} \cdot \frac{\beta_{235}}{\beta_{238}} \quad (5)$$

where the subscripts 235 and 238 refer to quantities associated with the 186 keV peak from ^{235}U and the 1001keV peak from ^{238}U . With Eq. 5, we can estimate the count ratio for a measurement of a uranium item of unknown enrichment. Evaluation of the four terms was done as follows.

1. We assume that the uranium items that we measure are not very young, such that the ratio of specific gamma-ray emissions for the 186-keV ^{235}U gamma ray and the 1001-keV $^{234\text{m}}\text{Pa}$ gamma ray remain invariant with time for any particular enrichment. Using our *GamGen* computer code [23], we computed these specific gamma ray emission rates for aged uranium at five enrichment grades [DU (0.2% ^{235}U), NU (0.7%), LEU (5%), HEU(20%), and WGU (93%)].

2. We measured gamma-ray standards of activity to determine the full-energy peak efficiency curves for HPGe detectors of 20%, 40%, 100%, and 170% relative efficiency at a distance of 1 meter. From these curves we determined the detector efficiencies for the 185.7- and 1001.03-keV full-energy peaks for the four detectors. At this distance, count rates fall off closely with the inverse square of the source distance even for somewhat extended sources. This is true for distances somewhat less than 1 meter and somewhat more for some field measurements. For this reason, we have assumed that the efficiency ratio is independent of source distance.
- 3.
4. With field measurements we can have no *a priori* knowledge of the presence and type of external absorbers, so we assume that none are present. This implies that $\alpha_{235}/\alpha_{238} = 1$ and that Eq. 5 becomes Eq. 6.

$$\frac{C_{235}}{C_{238}} = \frac{S_{235}}{S_{238}} \cdot \frac{\epsilon_{235}}{\epsilon_{238}} \cdot \frac{\beta_{235}}{\beta_{238}} \quad (6)$$

Differential attenuation through any absorbers that might actually be present would preferentially reduce the 185.7-keV full-energy peak. As a result we can, at best, only estimate a minimum value for enrichment.

5. We also can have no *a priori* knowledge of the nature of the uranium item that is being measured. As a result, an accurate estimate of self-absorption cannot be computed. It is likely that the greatest self-absorption would occur with pure uranium metal and that is our assumption. Further, if we assume that the item is represented by a line source placed along the detector axis, we can do a simple integration of exponential attenuation to determine the self-absorption of a uranium item of thickness, τ , which is likely to represent the maximum self-absorption that will be encountered. The integration leads us to Eq. 7.

$$\beta = A/A_0 = \frac{1}{\mu\tau} (1 - e^{-\mu\tau}) \quad (7)$$

where μ is the linear attenuation coefficient of the item material (cm^{-1}), A_0 is the total activity of the source and A is the activity measured when one end of the source is situated at the detector face. To choose a value of τ , we used Eq. 6 and 7 to compute the ratio of self-absorption in uranium for the 186- and 1001-keV gamma rays, as well as the ratio of the two, as a function of uranium thickness. These results are shown in Fig. 6.

In the figure there is a gentle “knee” at about 0.5 cm of uranium before the self-absorption ratio is dominated by ^{238}U . At 1.5 cm it is beginning to saturate so we set our value of τ at 1.5 cm, a substantial U thickness. We then computed Eq. 7 for the four detectors used for energy calibration to provide a rough estimate of the maximum range of self-absorption.

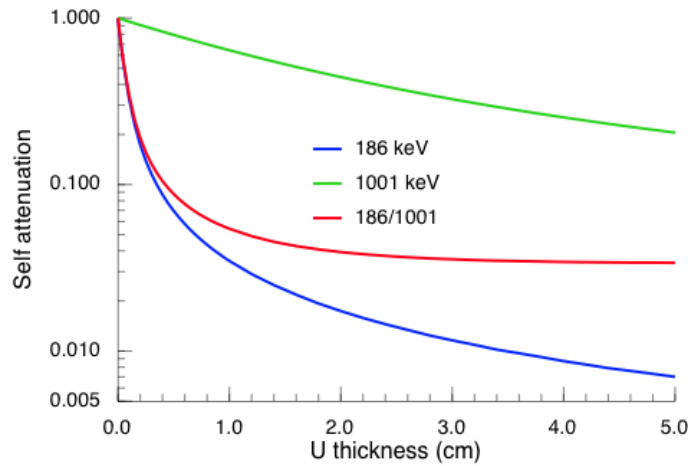


Fig. 6. Self-absorption of 185.7 and 1001.03-keV gamma rays and their ratio in uranium metal

Fig. 7 shows the results of the calculations for ²³⁵U concentrations of DU at 0.18%, natural uranium at 0.711%, LEU at 5%, borderline LEU/HEU at 20% and WGU at 93%. Using the computed self-attenuation ranges as a guide, and some empirical adjustments as a diversity of experimental results were obtained, we divided the count ratios into six count-ratio zones, that allow us to estimate minimum enrichment grade from measured 185.7/1001.03-keV count ratios. The vertical bars represent the self-attenuation range and result in overlap of some of the enrichment grade assignments, hence some ambiguity. The zone ranges and enrichment grade assignments are presented in Table 3.

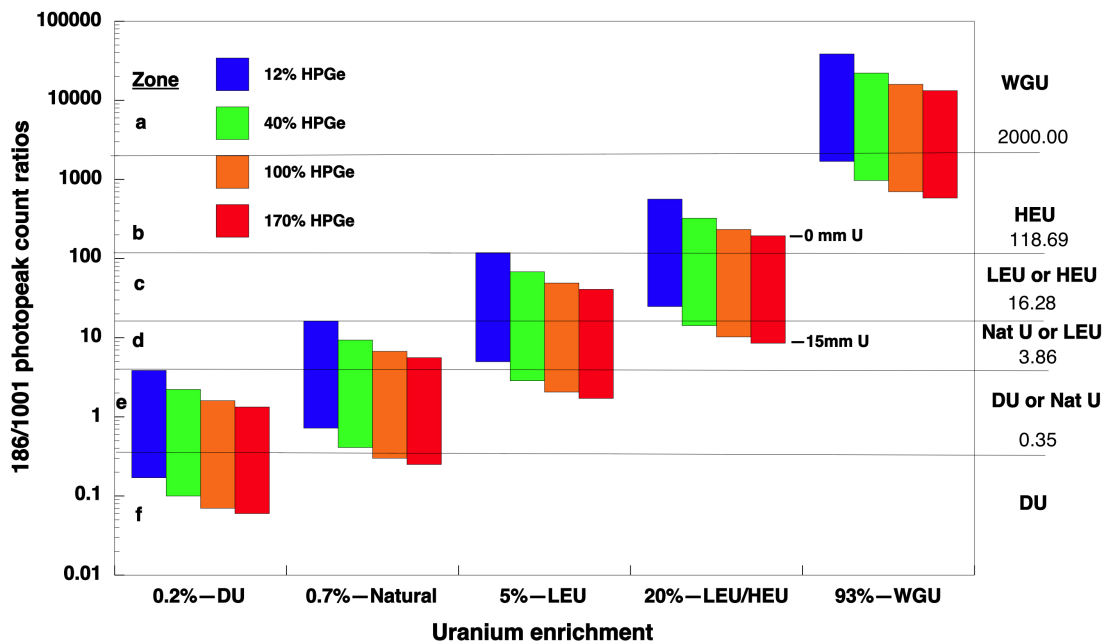


Fig. 7. 186/1001-keV photopeak ratio estimates for unshielded uranium as a function of enrichment, detector relative efficiency, and uranium thickness.

Table 3. Assignment of enrichment grade using zone boundaries defined in Fig. 7.

| Zone | Enrichment grade | 186/1001 count range |
|------|------------------|----------------------|
| f | DU | <0.35 |
| e | DU or NU | 0.35–3.86 |
| d | NU or LEU | 3.86–16.28 |
| c | LEU or HEU | 16.28–118.70 |
| b | HEU | 118.70–2000.00 |
| a | WGU | >2000.00 |

While self-absorption preferentially attenuates the 185.7-keV line, this is also true for external absorbers. Our self-absorption compensations extend over broad ranges of count ratios and are computed for self-absorption compensation only. Nevertheless, these broad ranges may be unintentionally helpful when external absorbers are present.

To test the utility of this approach we measured eight New Brunswick Laboratory (NBL) [5624] thin-window certified reference materials of uranium enrichment and compared the material's certified enrichment grades to the grades determined by *RadID*. These results appear in Fig. 8. The measurement results for the 186/1001-ratio for all of these standards fall neatly in the appropriate zones defined in Table 3. As the items increase in enrichment, we notice that they appear approximately linearly on the log-log plot up to 20%. As the enrichment increases, the 1001 peak counts begin to diminish rapidly and rapidly increase the peak ratio.

Fig. 17 shows results of essentially bare sources. Sufficiently shielded items with 186-keV counts diminished relative to 1001-keV counts would appear lower in the plot, falling into lower zones that would underestimate the enrichment.

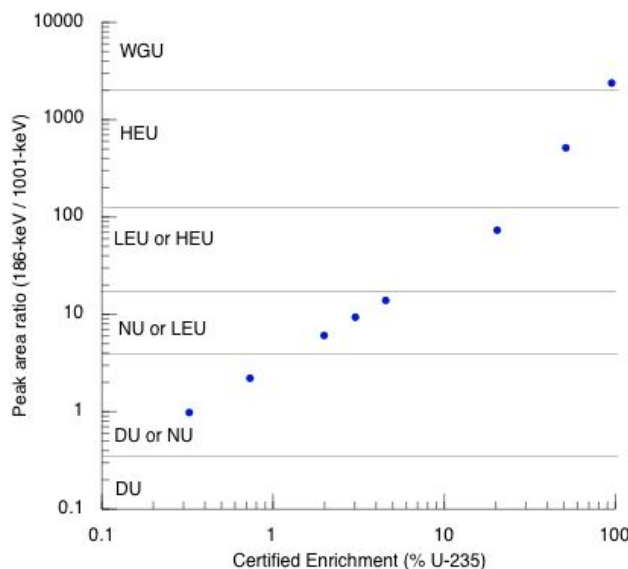


Fig. 8. A test of the enrichment grading by 186-keV/1001-keV peak area ratio. The blue symbols indicate measured ratios from New Brunswick Laboratory uranium enrichment standards are correctly graded according to Table 6.

Detecting HEU when no ^{238}U signal is manifest

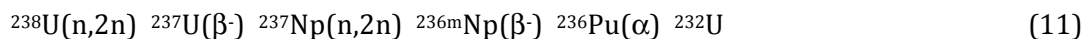
We analyzed a number of known WGU spectra in which the ^{238}U signature was not manifest to *RadID*. However, the ^{235}U signature in these spectra was manifest with strong 143-, 163-, 186-, and 205-keV lines. WGU spectra from other sources can have a considerably larger ^{232}U content, leading to a large Compton continuum from its daughter ^{208}Tl that masks the 1001-keV peak. Were these field spectra of unknown provenance then the measurement would be indicative that the measured items were lightly shielded. Light shielding and a strong ^{235}U signature combined with the absence of a manifest ^{238}U signature strongly suggest that the uranium is HEU with high ^{235}U content and, quite possibly, WGU.

Detecting shielded HEU

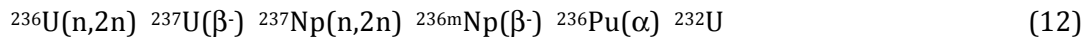
Because it can be used in the manufacture of nuclear explosives, illicit traffic in HEU is a matter of serious concern. Materials intervening between the detector and an HEU source will preferentially reduce the ^{235}U signal, eliminating or greatly reducing the ability to make roughly accurate enrichment estimates by the peak ratio method. An alternative surrogate HEU signature might be that of ^{232}U .

Uranium-232: grasping at straws to detect shielded HEU

With only a 69-year half-life, ^{232}U does not occur in nature but is introduced as a result of reactor irradiation of uranium resulting in a number of complex reaction and decay chains. Four of the most significant of these complex chains are [5725]:



Because uranium may contain ^{236}U as a result of the inclusion of previously reactor-processed uranium, another reaction chain may also be important:



In the 1960's, uranium that had previously been irradiated in reactors was introduced into U.S. gaseous diffusion plants to be re-enriched. Consequently, trace quantities of ^{232}U were entrained in the gaseous diffusion cascades where they remain today and became a minor contaminant in new feedstock as it was introduced to the cascade. It is believed that similar circumstances have occurred elsewhere. Evidence [5826] also suggests that, during the enrichment process, the ^{232}U is preferentially swept into the light isotope fraction that becomes HEU and immeasurably small amounts go into the heavy isotope fraction that becomes depleted uranium. Therefore, the manifest presence of ^{232}U in uranium is consistent with that uranium being HEU or, more likely, WGU.

The low energies and emission intensities of the gamma rays from decay of ^{232}U prevents it from being readily detectable directly. Consequently, we rely on yet another surrogate, ^{208}Tl , a distant radioactive daughter of ^{232}U (Fig. B-1) and a major contributor to the ^{228}Th signature in Fig. 6. The decay of ^{208}Tl results in the emission of several gamma rays with strong intensities. Of most interest is the highly penetrating gamma ray at 2614.53-keV with 99% emission intensity. While this gamma ray is readily detectable from HEU, its presence, however, is not unique, so that, without elimination of other possible sources of this radionuclide, it could lead to misidentification of shielded HEU.

Fig. 9 indicates the presence of ^{232}U at 2615-keV in a gamma-ray spectrum of WGU. The figure also illustrates this peak, from the Th decay series, in its background spectrum, scaled to the measurement time of the WGU spectrum, and taken when the WGU was absent from the laboratory. The 2615-keV peak in the gross spectrum of the WGU sample shows an excess of counts above background, by about a factor of three, that is attributable to ^{232}U .

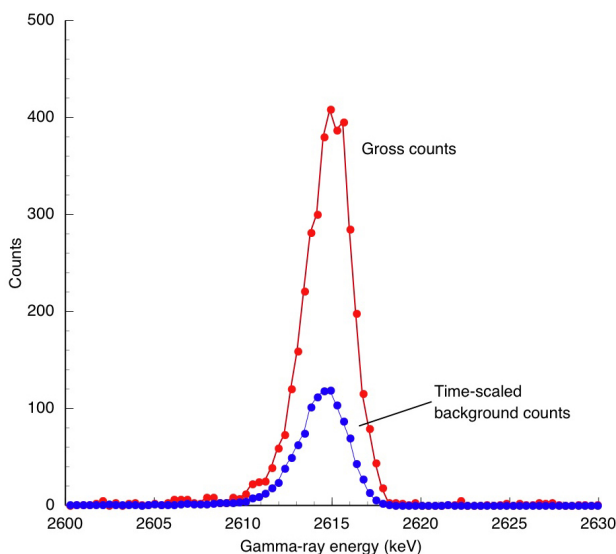


Fig. 9. The 2615-keV peaks in the spectra of background (blue) and the gross spectrum of WGU (red). The presence of ^{232}U is indicated by the excess counts above background in the WGU spectrum.

The simple fact that excess ^{232}U above background ^{232}U can be found in reprocessed uranium may be insufficient to infer that its presence alone is an indicator of the presence of shielded HEU. We may wonder if a shielding scenario could actually occur that would make an excess of the 2615-keV gamma ray a likely inference of shielded HEU. To investigate this, we did some simple computer simulations of two shielding variations, with results from of an old benchmark study to guide us.

Many years ago we did a benchmark study to accurately model the HPGe detector gamma-ray spectrum from thick actinide sources [27]. As part of that study we used an HPGe detector with 29% relative efficiency to acquire a spectrum from a 3.15 cm radius 93% ^{235}U sphere. And, subsequently, we measured a trustworthy overnight background

spectrum that we time-scaled and subtracted from the foreground spectrum to obtain a net spectrum that revealed the excess 2615-keV peak.

In the original study we modeled the sphere, with its declared isotopic vector (except for ^{232}U), and its environs in detail with the MCNP 3-D Monte Carlo code [6028] to obtain the gamma-ray flux at the detector face. We then convolved those results with a full-spectrum response function for our detector, determined with the method of Mitchell [29], to obtain a highly accurate simulation of the HPGe spectrum. Using this simulation we were able to determine the isotopic fraction of ^{232}U at 0.100 ± 0.001 ppb.

For this paper, we modeled the bare sphere with a 1-D-spherical deterministic code using a reasonable facsimile of the original geometry, the declared uranium isotopic vector, and the ^{232}U isotopic value determined by the original benchmark study. The modeled flux at the detector was convolved with a detector response model that we had on hand for a detector of 20% relative efficiency.

This was followed by two more models with Pb cladding to study the effect of the 186/1001 peak-count ratio as a function of cladding thickness. If the sphere is shielded to avoid detection, the choice of lead as the shielding material is not entirely arbitrary. The desired criteria for such a shield would be high-Z, high density, low expense, easy obtainability, and, perhaps a low melting temperature for casting. Lead satisfies all of these criteria.

To estimate how much cladding would be needed to reduce the 186/1001-count ratio from bare 93% WGU to an apparent 20% borderline ^{235}U HEU content value, we rearranged and repurposed Eq. 5 to study external shielding rather than self-absorption.

$$\frac{C_{235}}{C_{238}} = \frac{S_{235}}{S_{238}} \cdot \frac{\epsilon_{235}}{\epsilon_{238}} \cdot \frac{\beta_{235}}{\beta_{238}} \cdot \frac{\alpha_{235}}{\alpha_{238}} \quad (13)$$

Because we are using the same sphere in every simulation, the specific gamma-ray emission rates are constant as are the self-absorption terms. Further, because we are using the same detector for every simulation, the efficiency ratio remains constant. Therefore Eq. 13 reduces to Eq. 14.

$$\frac{C_{235}}{C_{238}} = k \cdot \frac{\alpha_{235}}{\alpha_{238}} \quad (14)$$

where k is a constant of proportionality. We now return to our model of a line source placed along the detector axis and Eq. 14 becomes Eq. 15.

$$\frac{C_{235}}{C_{238}} = k \cdot \frac{e^{-\mu_{235}x}}{e^{-\mu_{238}x}} \quad (15)$$

Where the μ -values are the linear attenuation coefficients for 186- and 1001-keV gamma rays in Pb and x is the Pb thickness. We note that when the material is bare, $x = 0$, the exponential term is unity, and k is the count rate ratio. We have measured the count rate ratios for standards of 20%- and 93%-material (Fig. 8) with a portable HPGe detector and found the k -values to be 74 and 2388. We inserted these values into Eq. 15 and computed

the count rate ratio for these two enrichments as a function of Pb thickness as shown in Fig. 10.

With increasing Pb cladding, the count rate ratio descends exponentially. With a cladding of 2.4 mm, the count ratio for WGU is roughly equal to that of bare uranium of 20% enrichment. Using the uranium isotopic vector of the sphere (0.1 ppb ^{232}U , 1.00% ^{234}U , 93.30% ^{235}U , 0.60% ^{236}U , and 5.10% ^{238}U), we computed our HPGe spectral simulations for bare WGU and for WGU with 2.4 mm Pb cladding. These are shown in Fig. 20 overlaid on the original net measured spectrum for comparison.

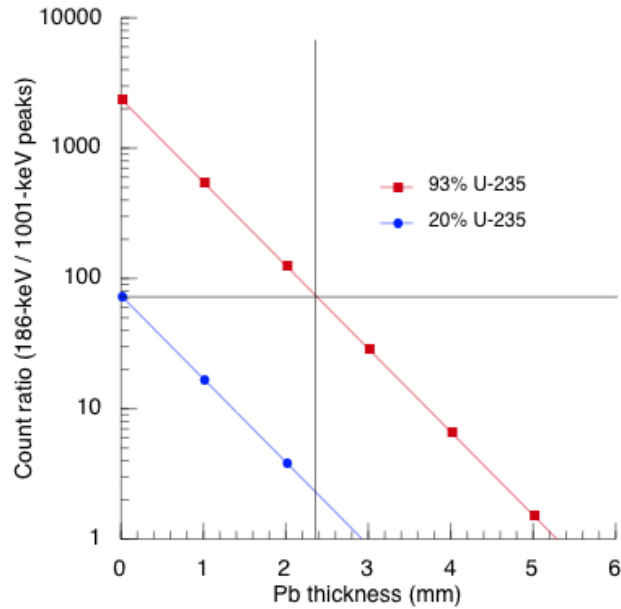


Fig. 10. The approximate expected 186- to 1001-keV peak count ratio as a function of Pb cladding thickness over a WGU sphere. The crosshairs indicate the WGU count ratio when it descends as a function of cladding thickness to the value equivalent to a bare sphere of 20% uranium enrichment and its corresponding Pb thickness of about 2.4 mm at this count ratio.

Fig. 11 shows the 1-D models of the HPGe spectrum from a WGU sphere superimposed on the net measured spectrum and scaled slightly for registration with the measured spectrum at 186 keV. We included the measured net spectrum from the old study as a qualitative check on the new computation. The older spectrum was taken with a more efficient detector and exhibited less downscatter, particularly at low energies. In the computed spectra, the expected dramatic reduction in counts at low energies appears and only the modest expected reduction at higher energies.

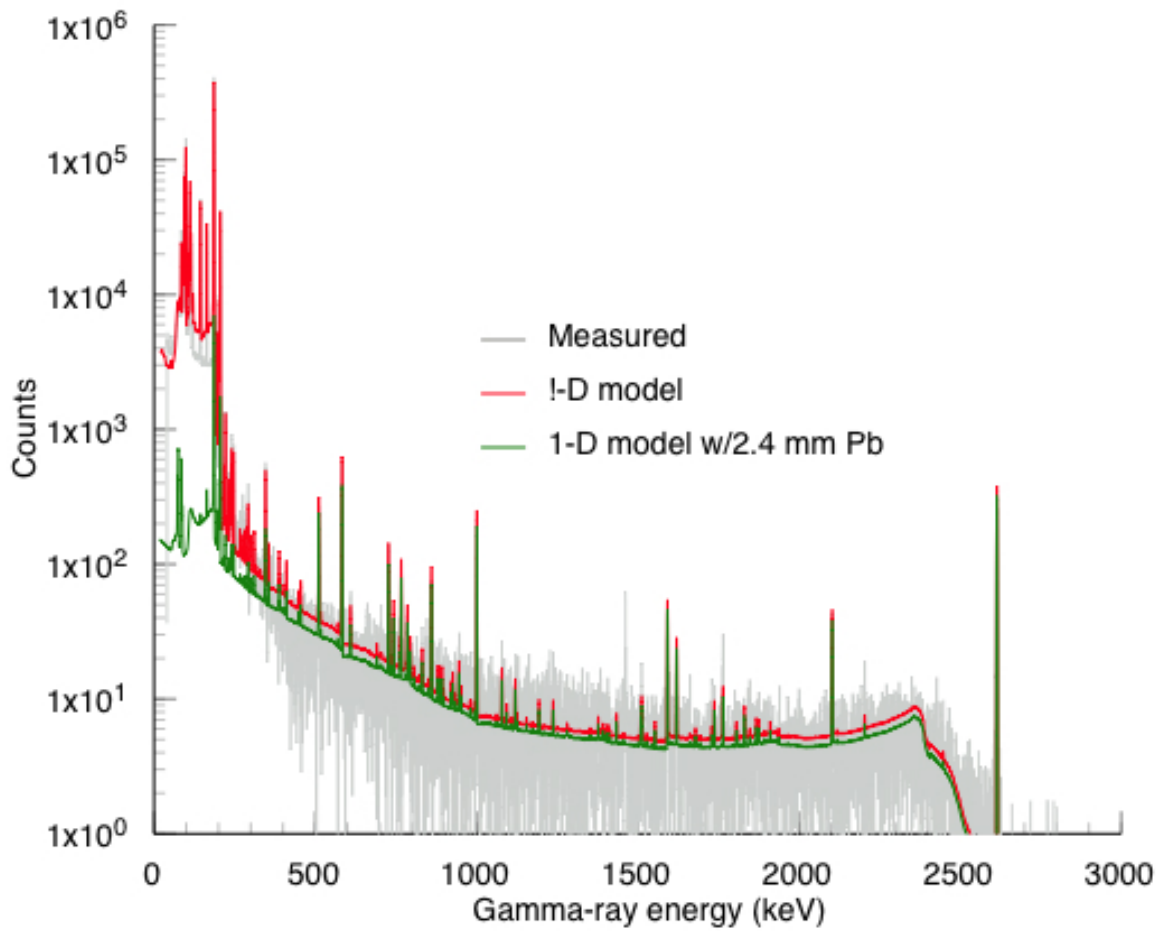


Fig. 11. 1-D models of the HPGe spectrum from a WGU sphere superimposed on a net measured spectrum. The unshielded 1-D model closely conforms to the measured spectrum with greater downscatter at low energies. The 1-D model with 2.4 mm Pb cladding shows a dramatic drop in low-energy counts and modest decreases at higher energies.

In Fig. 12 we expanded the low-energy portion of Fig. 11 for a closer examination.

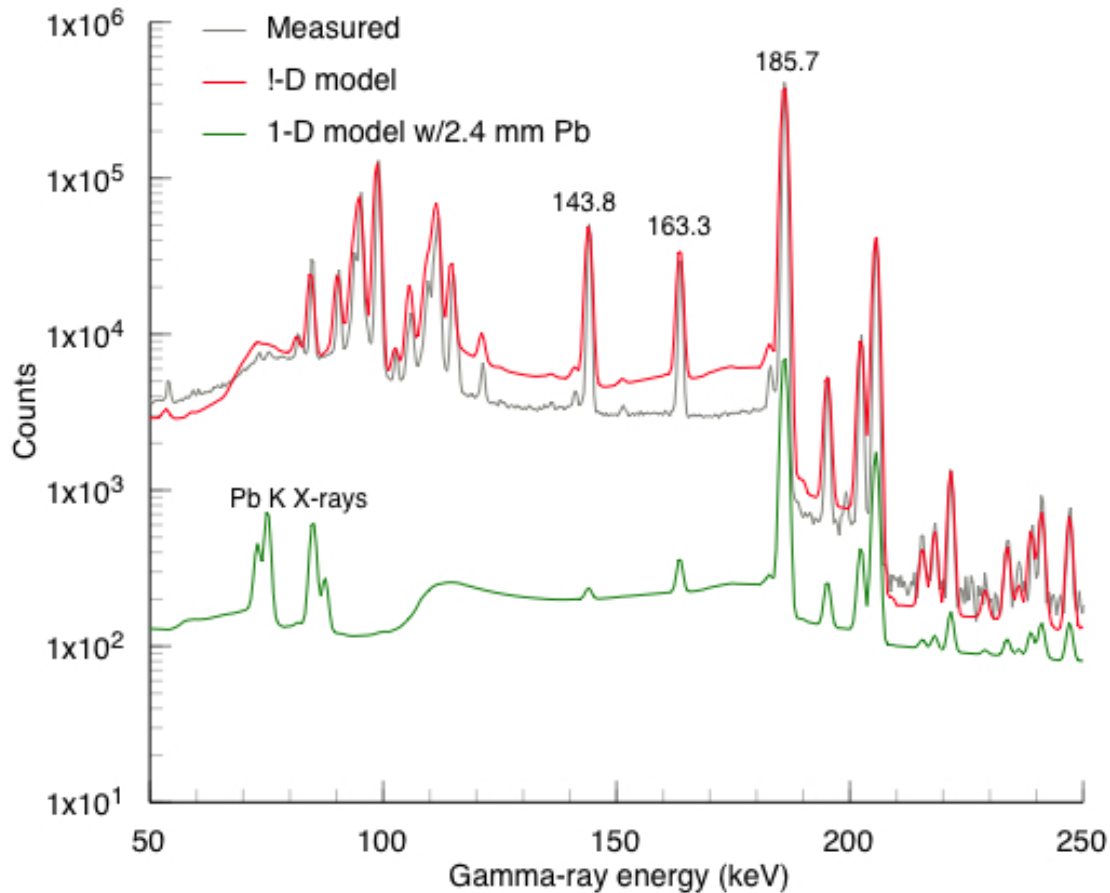


Fig. 12. Expanded view of the low-energy portion of the spectral plots in Fig. 11. The 1-D model indicates the increased downscatter in the modeled smaller detector. When the 2.4 mm Pb cladding was added, the spectrum was attenuated about two orders of magnitude in this region. Complete attenuation of the Th K X-rays and low-energy ^{235}U peaks and the 120.9-keV peak from ^{234}U has occurred. Pb X-ray fluorescence stimulated by ^{235}U radiation indicates the presence of the Pb cladding.

RadID analyses of the computed spectra indicate that the unshielded model is WGU and the model with 2.4 mm shielding was determined to be “U-235, LEU or HEU or shielded WGU,” consistent with the fact that 20% enrichment is borderline between LEU and HEU. A second model computed with 3 mm Pb cladding (not shown) and analyzed with *RadID* correctly gave the result “U-235, NU or LEU weak or shielded.” In both cases, the ^{235}U signature was manifest and would invite very close scrutiny by nuclear incident responders.

What can we learn from Figs. 11 and 12?

1. A thin shield (2.4 mm Pb) will reduce the 185.7-keV peak height by about a factor of 50 but the ^{235}U signal is still manifest. Doubling the cladding thickness would reduce the 185.7 keV peak by another factor of about 50.
2. Severe differential attenuation of the four principal ^{235}U peaks at 143.2-, 163.4-, 185.7-, and 201.3-keV, is quite evident in Fig. 12. Of these, the two most likely to be manifest and testable in a like shielding situation, are the peaks at 185.7- and 205.3-keV.
3. The presence of the Pb cladding was announced by the Pb K-series X-ray fluorescence and provides further credence of significant shielding.

Nevertheless, our model is unrealistic in a number of ways:

1. It does not include background radiation.
2. It is deterministic and doesn't include statistical "jitter."
3. It was convenient to use known data to generate the model but the original sphere is unrealistically small with a mass of only 2.2 kg, while the IAEA significant quantity for HEU ($^{235}\text{U} \geq 20\%$) is 25 kg [30]. A 25 kg uranium sphere would increase the ^{235}U signature strength by about a factor of 7.
4. A less unrealistic model would be a 25 kg sphere. A 10 mm Pb-clad would only add about 2.5 kg to the mass, not likely an undue penalty.
5. Furthermore, a variety of other geometries and shielding could be used.

Beyond these obvious considerations, if this issue merits a more thorough study, our simple model is clearly insufficient.

Distinguishing between ^{232}U and ^{232}Th

Just what can be inferred from the presence of ^{228}Th in a gamma-ray spectrum is quite ambiguous. The most likely inference is that it is from background radiation (i.e. that portion originating from ^{232}Th). The second most likely is that it is from NORM or TENORM containing ^{232}Th . For example, thorium metal is also used as a hardener for magnesium alloys. A tungsten alloy with 2% thorium [6231] is used for welding electrodes. Thorium oxide is a constituent of some optical glasses. Rarely encountered nowadays are gas lantern mantles infused with thorium nitrate.

A distinguishing signature for ^{232}Th that has aged a month or more since chemical purification are gamma rays, particularly at 911-keV (Fig. C-2) emitted in the decay of its granddaughter ^{228}Ac . Because ^{232}U is located in a collateral decay series that converges with the thorium decay series at ^{228}Th (Fig. B-X), ^{228}Ac is not one of the daughters of ^{232}U . The presence of the 911-keV gamma ray is therefore a telltale that indicates presence of ^{232}Th and not ^{232}U .

As a further caution, we note that the production of TENORM, as in the case of gas lantern mantles, can entail some chemical purification of thorium which results in the presence of ^{228}Th but not, at least initially, ^{228}Ac with its telltale 911-keV gamma ray. This is because before subsequently decaying to ^{228}Ac , it takes a while before sufficient ^{228}Ra has

decayed so that enough of its daughter ^{228}Ac has accumulated to make its 911-keV gamma ray manifest. So, an identification of ^{228}Th , without the 911-keV gamma ray, would only inconclusively be indicative of the presence of ^{232}U .

Here is at least one case in which background radiation has an important use, that is to determine that the ^{208}Tl in the foreground spectrum is in excess above background and might be attributed to ^{232}U as an indication of the presence of HEU or even ^{233}U . If this criterion is satisfied, however, it must be kept in mind that the excess ^{208}Tl signature is possibly from young ^{232}Th .

Further distinguishing between natural U and processed U

An important characteristic that we investigate is whether the uranium being measured is natural or processed material. If we've already established that the uranium enrichment determination by *RadID* is not natural but is unambiguously DU or LEU or higher, then it has obviously been processed and the methods discussed here will be supplementary. If our Peak-area enrichment estimate falls in the ambiguous zones (DU or NU) or (NU or LEU) in Table 6, we may still be able to distinguish between processed and unprocessed uranium by examining selected ^{238}U daughter full-energy-peak ratios.

The 609/1001 peak-area ratio

As already noted, significant ingrowth of $^{234\text{m}}\text{Pa}$ in processed uranium occurs in only a few weeks. Decay of $^{234\text{m}}\text{Pa}$ produces gamma rays at 1001.03- and 766.38-keV that provides the most significant signature for the presence of ^{238}U . In the foreground spectra from natural uranium, the most intense gamma ray from the distant daughters of ^{238}U is the 609.31-keV peak following the decay of ^{214}Bi . The 1001-keV peak also appears from background radiation but may be too weak, in a given spectrum, to be manifest. As a result we can expect that the ratio of the counts in the 609-keV peak to the counts in the 1001-keV peak from the decay of $^{234\text{m}}\text{Pa}$ in processed uranium to be high if determinable at all.¹ This is reflected in the blue bar measurement results in the 609/~~1001~~-1001-column in Fig. 13.

In a foreground spectrum from processed uranium, the 609-keV peak will only be present from background ^{214}Bi as the long half-life of ^{234}U (Fig. A-1) significantly retards sufficient ingrowth of the distant ^{238}U daughters in processed uranium for decades. The 1001-keV peak that appears weakly in background radiation is enhanced relative to the 609-keV peak with the presence of a processed uranium source. As a result the ratio of the 609-keV peak to the 1001-keV peak in processed uranium can be expected to be lower than in natural uranium as reflected in the brown bar measurement results in Fig. 13.

¹ *RadID* can only compute a peak-area ratio when both of the peaks are manifest; otherwise the ratio is indeterminable.

The 1001/766 peak-area ratio

Because the 766-keV and 1001-keV peaks are emitted by the same nuclide, we would initially expect that this ratio would be constant. However, as illustrated in Fig. 2, in natural uranium radiation, the 766.41 ^{234m}Pa peak forms a doublet with the 768.38-keV peak from ^{214}Bi . We integrate the counts in the doublet to substitute for the 766-keV peak alone. This leads to a considerably increased ratio value that allows us to discriminate between natural and processed uranium. Data from the same four spectra used to compute the 609/1001-ratio for natural material produced the blue bar in the right-hand column of Fig. 22.

Determinable values of this ratio from available foreground measurements of *processed* uranium were obtained mostly from DU to LEU material, as both the 1001- and 766-keV peaks are relatively weak in highly enriched material. The short brown bar in the right-hand column of Fig. 13 represents the extent of 14 measurements of *processed uranium*, three of which were used to produce the 609/1001-ratio result. The spread in the expected constant value is from wide variation in counting statistics

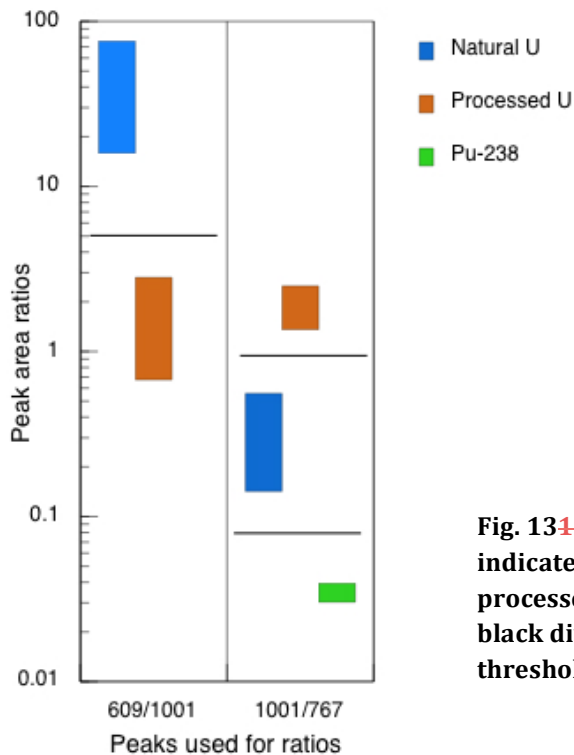


Fig. 131. Ratios of gamma-ray lines that can indicate whether uranium is natural or processed or whether ^{238}Pu is present. The black dividers in the figure indicate the threshold values used for testing the ratios.

conclusion

Uranium in its variety of forms, enrichments, and appearance in two reactor fuel cycles presents a challenge to rapidly and unambiguously identify its presence and its qualitative attributes from field measurements. We led the reader along selected pathways in the labyrinth of actinide element creation and decay, pausing to examine the salient radiation signatures of the uranium isotopes, their daughters, and others that can interfere with uranium detection and characterization. We developed a method to make approximate estimates of minimum uranium enrichment and briefly explored the effect of cladding on HEU.

Acknowledgement

RadID is the descendent of a simple radionuclide identification code for HPGe detectors that was the brainchild of Mark S. Rowland and was implemented in software by James L. Wong.

Appendix A: The uranium decay series

The radiation signatures of natural and processed uranium in gamma-ray spectra can be understood and distinguished by the decay of ^{238}U and, importantly, by its radioactive daughters. Uranium-238 is the progenitor of a long radioactive decay series. A diagram with the main features of the uranium series is shown in Fig. A-1.

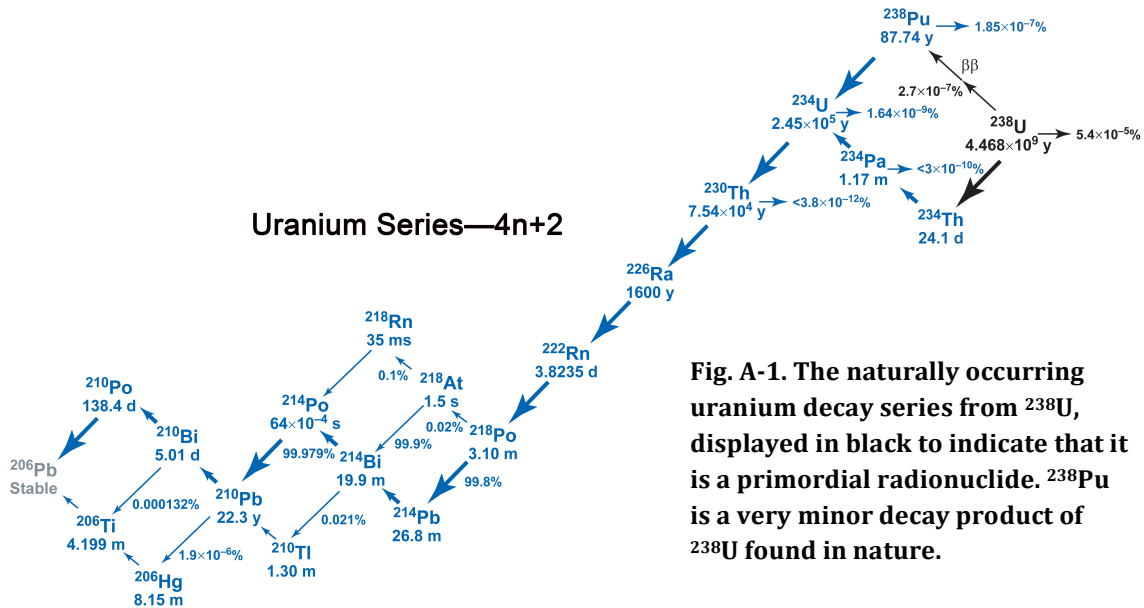


Fig. A-1. The naturally occurring uranium decay series from ^{238}U , displayed in black to indicate that it is a primordial radionuclide. ^{238}Pu is a very minor decay product of ^{238}U found in nature.

The figure illustrates that the intermediate nuclides in the series have short half-lives in comparison to uranium-238². If a uranium-bearing system is left undisturbed for a few million years, a state of secular (long-term) equilibrium becomes established. In this case, the activities of all of the daughter nuclides are equal to the ^{238}U activities. However, during geological processes such as erosion, sedimentation, melting, or crystallization, different nuclides in the decay series can become fractionated relative to one another, due to variations in their chemistry or the structural site they occupy [32].

When making gamma-ray measurements in the field, we encounter natural uranium in two forms. The first is that gamma-ray field measurements, include some background radiation, in which ^{238}U and its daughter nuclides contribute significantly. Background radiation is ubiquitous, diffuse, and very low-level but can act as an interference with measurements of weak radioactive sources. The second natural uranium form, occasionally encountered in commerce, is uranium ore.

² These short half-lives are useful for dating Pleistocene geological events that are too old to be well resolved by radiocarbon dating and too young to be well resolved by methods employing longer half-lives [32]

Appendix B: The thorium decay series

Before we examine the gamma-ray spectra of background and uranium ore, we need to consider the other two sources besides the uranium series that contribute substantially to the structure of background spectra. The first of these is ^{40}K , a primordial radionuclide found in all potassium and is ubiquitous in the environment. A single 1460.8-keV gamma ray is emitted following the electron-capture decay of ^{40}K . Another major source of structure in background spectra is from the thorium decay series shown in Fig. B-1. The figure also includes ^{232}U , a man-made byproduct of plutonium production, and ^{236}Pu , that are discussed in the following section on uranium enrichment.

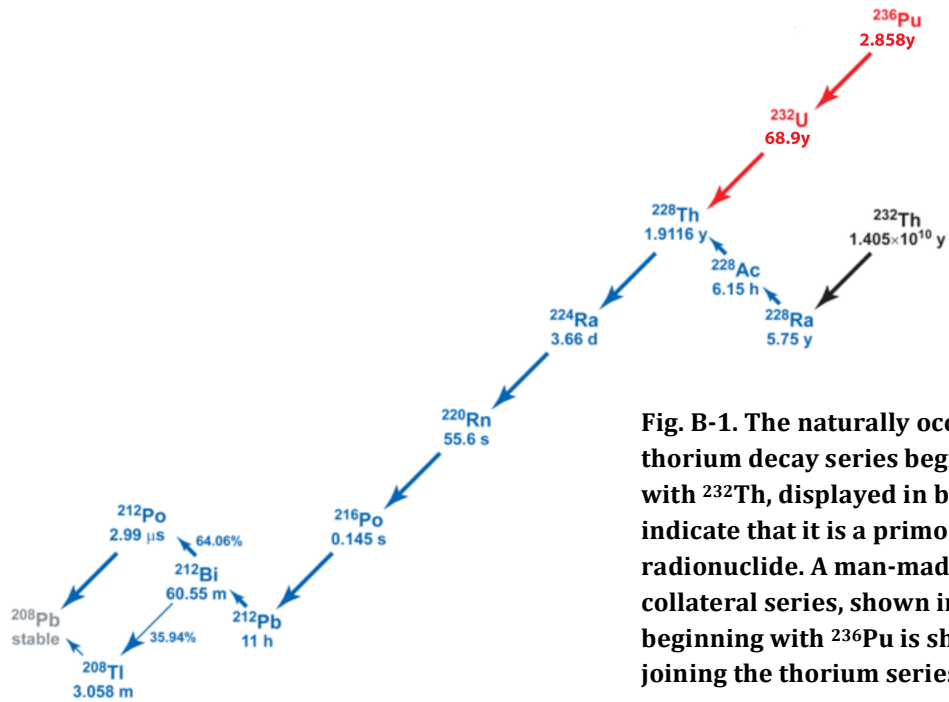


Fig. B-1. The naturally occurring thorium decay series beginning with ^{232}Th , displayed in black to indicate that it is a primordial radionuclide. A man-made collateral series, shown in red, beginning with ^{236}Pu is shown joining the thorium series at ^{228}Th .

Thorium-228: Nexus nuclide—a ubiquitous and ambiguous signature

The natural thorium decay series arises from the decay of the 1.4×10^{10} -y primordial radionuclide ^{232}Th . Thorium-228, with a 1.9-y half-life, is the great granddaughter of ^{232}Th . It decays to seven successive radioactive daughters. These daughters are so short-lived that they require the presence of the longer-lived ^{228}Th to sustain their existence for more than a few weeks. One of these daughters, ^{208}Tl , provides one of the most recognizable signatures in background radiation with strong gamma rays at 583-, 861-, and 2615-keV. Observation of ^{208}Tl , therefore, almost always indicates the presence of ^{228}Th . A computer-simulated point-source ^{228}Th spectrum is shown in Fig. B-2 illustrates its gamma-ray signature.

The importance of ^{228}Th is that it is the nexus of two decay series with the nuclides, ^{232}Th , ^{232}U , and ^{236}Pu as their progenitors (Fig. B-1). The presence of ^{228}Th in a gamma-ray spectrum is therefore not unique to a particular parent, which can make it a problematic but sometimes useful signature. Table B-1 illustrates source types that produce ^{228}Th and their

parents. The presence of ^{202}Tl and its significance in these source types is discussed separately.

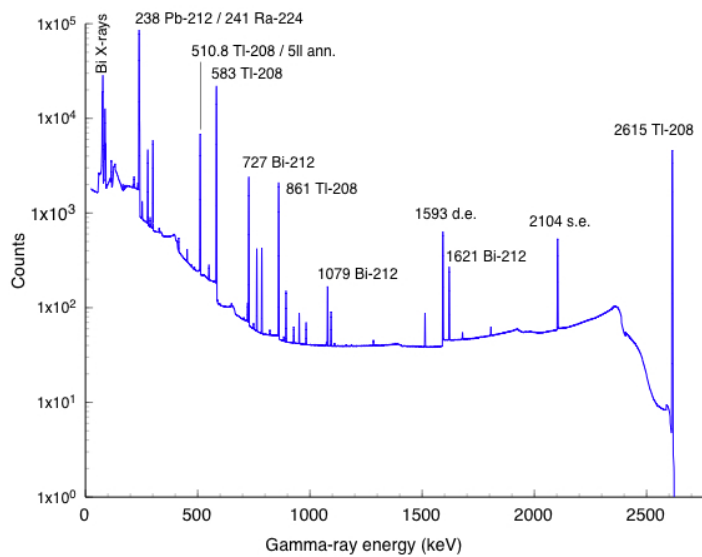


Fig. B-2. Illustration of the ^{228}Th signature with a computer-simulated HPGe spectrum from a year-old ^{228}Th point source

Table B-1. Source types exhibiting a ^{228}Th signature

| Source Type | ^{228}Th parent nuclide |
|---|----------------------------------|
| Background radiation | ^{232}Th |
| TENORM consumer products [33] | ^{232}Th |
| HEU and WGU | ^{232}U |
| ^{233}U | ^{232}U |
| Heat-source Pu | ^{236}Pu |
| Pu graded by ^{240}Pu content [55] | |
| Weapons-grade Pu (<7% ^{240}Pu) | ^{236}Pu |
| Fuel-grade Pu (7% \geq ^{240}Pu <19%) | ^{236}Pu |
| Reactor-grade Pu (19% ^{240}Pu and greater) | ^{236}Pu |

Appendix C: About uranium

Volumes have been written about uranium. Here we concentrate on those aspects of uranium that can be revealed by rapid automatic nuclide identification and attribution by high-resolution gamma-ray spectrometry.

Natural uranium

Uranium is a primordial radioactive element found in trace amounts in all rocks and soil, in water and air, and in materials made from natural substances. Nevertheless, it is one of the more common elements in the Earth's crust, roughly some 40 times more common than silver and 500 times more common than gold [34,35,36].

Uranium appears naturally in the form of a vector of three isotopes, ^{234}U , ^{235}U , and ^{238}U . By mole fraction their natural isotopic abundances are 0.000054(5) for ^{234}U , 0.007204(6) for primordial ^{235}U , and 0.992742(10) for primordial ^{238}U [37] but variation does exist in uranium isotope ratios (for example, [38]). Uranium-234 is not primordial but appears as one of the decay daughters of ^{238}U .

Uranium ore

While uranium typically occurs in trace amounts in the earth's crust, it is also found concentrated in a range of minerals [39,40,41]. Some are quite beautiful and a few are found in extensive deposits that are economically recoverable—these are the uranium ores.

Uranium occurs in nature as a mixture of numerous uranium oxides. The most common forms of uranium oxide are triuranium octaoxide (U_3O_8) and uranium dioxide (UO_2). Triuranium octaoxide is the most common form found naturally and can remain in the soil for thousands of years without moving downward into groundwater [42]. Both oxide forms are solids, have low solubility in water, and are relatively stable over a wide range of environmental conditions.

Unsurprisingly, both triuranium octaoxide and uranium dioxide are commonly found in uranium ores [43,44]. The two primary uranium ores are uraninite and pitchblende. Uraninite contains both UO_2 and U_3O_8 , with UO_2 dominating. Uraninite usually forms black, gray, or brown crystals that are moderately hard and generally opaque. A variety of uraninite ore that is dense and found in granular masses with a greasy luster is called pitchblende, in which U_3O_8 dominates [45].

Enriched uranium

Fluorine in uranium—Uranium hexafluoride and uranyl fluoride

During uranium processing, milled uranium ore—or yellowcake (principally triuranium octaoxide, U_3O_8)—is chemically processed to produce uranium hexafluoride (UF_6). Uranium hexafluoride is used in both of the main uranium enrichment methods, gaseous diffusion and the gas centrifuge method. Uranyl fluoride (UO_2F_2) is an intermediate compound in the conversion of UF_6 to a uranium oxide or metal form [46].

In both UF_6 and UO_2F_2 , uranium, an alpha particle emitter, is in intimate contact with fluorine that is then subject to both $^{19}\text{F}(\alpha, n)^{22}\text{Ne}$ and $^{19}\text{F}(\alpha, p)^{22}\text{Ne}$ reactions. Both reactions populate the 1274.53-keV excited state of ^{22}Ne that emits a gamma ray of that energy shown in Fig. C-1. We do not currently have access to a spectrum of UF_6 but it is reasonable to expect that a 1275 keV peak could also be manifest in UF_6 .

The 1275 keV gamma ray is the same gamma ray emitted by commonly used ^{22}Na calibration sources. However the common presence of uranium in a spectrum and a 1275 keV gamma ray is a likely signature for uranium in the midst of processing.

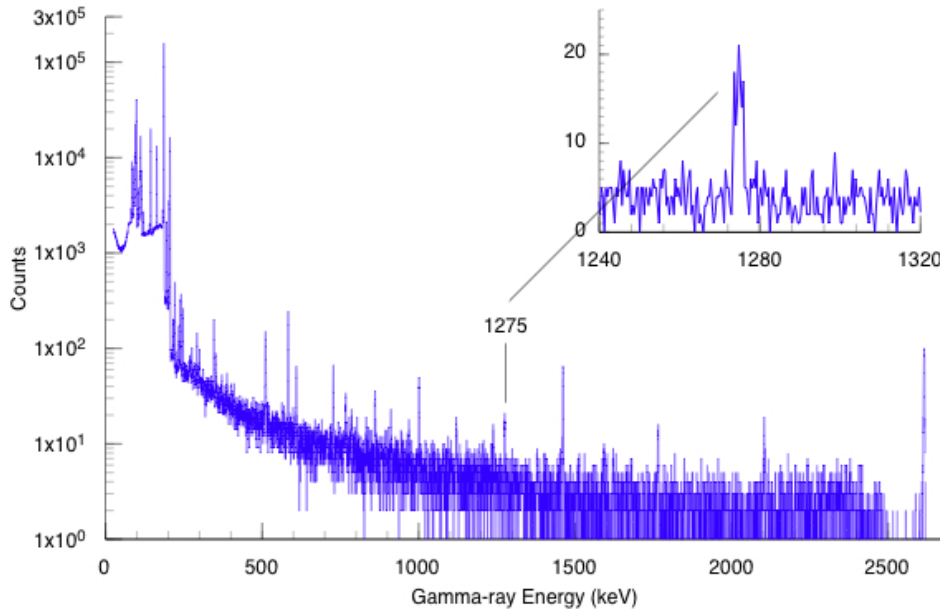


Fig. 1C-1. Gamma-ray spectrum of enriched uranium residue, including uranyl fluoride, showing the 1275-keV peak emitted following alpha-particle activation of ^{19}F .

When processed, uranium is chemically purified, removing the daughters of ^{235}U and ^{238}U , except for its ^{234}U daughter. Processed uranium is typically enriched in the isotopic fraction of ^{235}U . If not enriched, the processed uranium can be made into heavy-water reactor fuel. It will have retained its natural isotopic vector and, although processed, is confusingly referred to as natural uranium (NU). The tailings of the enrichment process, depleted uranium (DU), are reduced in their ^{235}U content. Uranium enrichment grades are shown in Table C-1.

Table C-1. Uranium enrichment grades

| Grade | Percent ²³⁵ U | Typical uses |
|--|--------------------------|--|
| Depleted uranium (DU) | <0.711 [47] | Radiation shielding, armor-piercing bullets, ballast |
| Natural uranium (NU) | 0.711 [47] | Heavy-water reactor fuel |
| Low-enriched uranium (LEU) | 0.711% < LEU < 20% [47] | Light water reactor fuel |
| Highly enriched uranium (HEU) | >20% [47] | Naval and fast neutron reactor fuel, medical radionuclide production |
| Weapons-grade uranium (WGU) ³ | >85–90% [48,49] | Nuclear explosives, Naval reactor fuel [50] |

Reprocessed uranium

Reprocessed uranium (RepU) is the uranium recovered from nuclear reprocessing, as done commercially in France, the UK, Japan, and by nuclear weapons states' military plutonium production programs. This uranium actually makes up the bulk of the material separated during reprocessing. Commercial light-water reactor spent fuel contains on average (excluding cladding) only four percent plutonium, minor actinides, and fission products by weight. Reuse of reprocessed uranium has not been common because of low prices in the uranium market of recent decades, and because it contains undesirable isotopes of uranium [25].

During its irradiation in a reactor, uranium is profoundly modified. The uranium that leaves the reprocessing plant contains all the isotopes of uranium between ²³²U and ²³⁸U. Uranium-237, with only a 6.75-day half-life, decays rapidly to ²³⁷Np [8].

The composition of reprocessed uranium depends on the initial enrichment and the time the fuel has been in the reactor [52]. A typical vector of uranium isotopes in reprocessed uranium, with attributes, is listed in Table C-2.

³ This designation is an unofficial subset of HEU but is in widespread use.

Table C-2. Typical isotopic vector of reprocessed uranium [51]

| Isotope | Proportion (%) | Half-life | Characteristics |
|------------------|----------------|-----------|--|
| ^{238}U | 99 | 4.47e9 y | Fertile material |
| ^{237}U | ~0.001 | 6.75 d | Decays rapidly to ^{237}Np |
| ^{236}U | 0.4–0.6 | 2.34e7 y | Neutron absorption lowers reactivity, also produces ^{237}Np |
| ^{235}U | 0.4–0.68 | 7.04e8 y | Fissile material |
| ^{234}U | >0.02 | 2.46e5 y | Fertile material, neutron absorption increases reactivity |
| ^{233}U | trace | 1.59e5 y | Fissile material |
| ^{232}U | trace | 68.9 y | Decay product ^{208}Tl emits strong gamma radiation making handling difficult |

The uranium contribution to background spectra

The HPGe background spectrum in Fig. C-2 was accumulated for nearly 18 days to reveal many of the background peaks that are not observed in shorter counting intervals⁴. The uranium ore spectrum in Fig. 7 was accumulated for 564 s live time. To isolate and emphasize the structure of the ore spectrum, we present it as a “net” spectrum; a reliable background spectrum was taken immediately after the foreground spectrum and subtracted on a channel-by-channel basis. In this spectrum there are 50 or more manifest peaks. The majority of the peaks are from decay of the distant ^{238}U daughter ^{214}Bi . Next in number are photopeaks from ^{214}Pb and a single peak from ^{226}Ra at 186.2-keV. Save for the ^{226}Ra peak itself, all of these are ^{226}Ra daughters. Were it not for the presence of the $^{234\text{m}}\text{Pa}$ 1001-keV peak, they would represent a spectrum of pure ^{226}Ra such as used medically for brachytherapy and, in the past, on radioluminescent watch and instrument dials [53]. Comparing the background spectrum to the net uranium ore spectrum, we see the ^{40}K peak at 1461-keV, ^{214}Pb peaks, and peaks from nuclides in the thorium series, notably ^{228}Ac and ^{208}Tl .

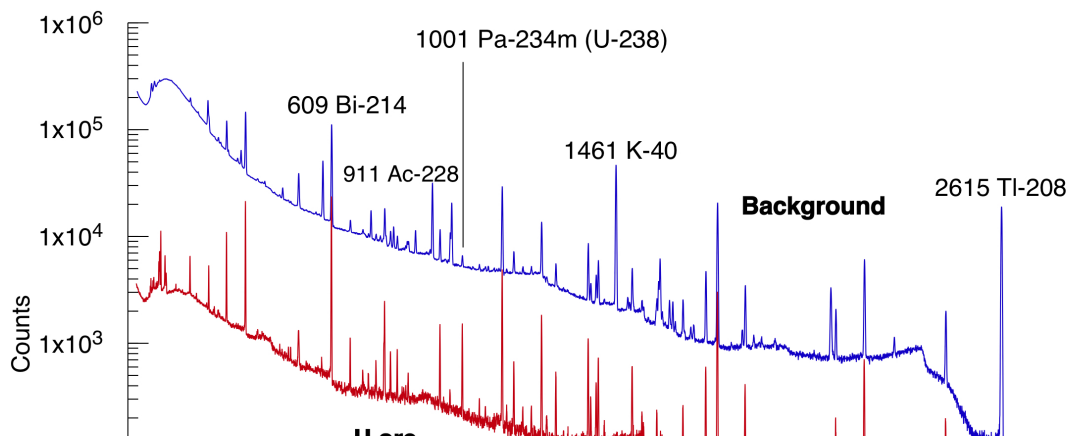


Fig. C-2. Gamma-ray pulse-height spectra of background and uranium ore taken with HPGe detectors of 20% nominal relative efficiency [54]. The background spectrum was accumulated for 1.532×10^6 s, or about 18 days. The ore spectrum was accumulated for 564 s live time at 100 cm with 13% dead time. A background spectrum, taken after the foreground spectrum, was subtracted to produce a net ore spectrum. The same natural uranium peaks appear in the background spectrum where the contributions from ^{40}K and ^{232}Th decay are also apparent. Some of the most prominent background peaks are called out for subsequent discussion.

Because of its strong presence in background, in some circumstances background uranium radiation could largely mask the presence of a uranium ore signature. However, because uranium is usually a diffuse trace element in the earth's crust, internal conversion following alpha decays of the uranium isotopes results in thorium K X-ray emissions that are usually too weak in background to be reliably observed. In the case of uranium ore, however, the decay of $^{234\text{m}}\text{Pa}$ to ^{234}U results in the emission of characteristic uranium K X-rays. These appear in the 95–115 keV region. The strongest of these is the K_{α_1} X-ray at 98.44 keV and the K'_{β_1} ($K_{\beta_1} + K_{\beta_3} + K_{\beta_5}$) peak at 111 keV that are an observable tell for the presence of lightly or unshielded uranium ore. This X-ray signature is visible in Fig. C-2 and more clearly in an expanded view of the low-energy region in Fig. C-3.

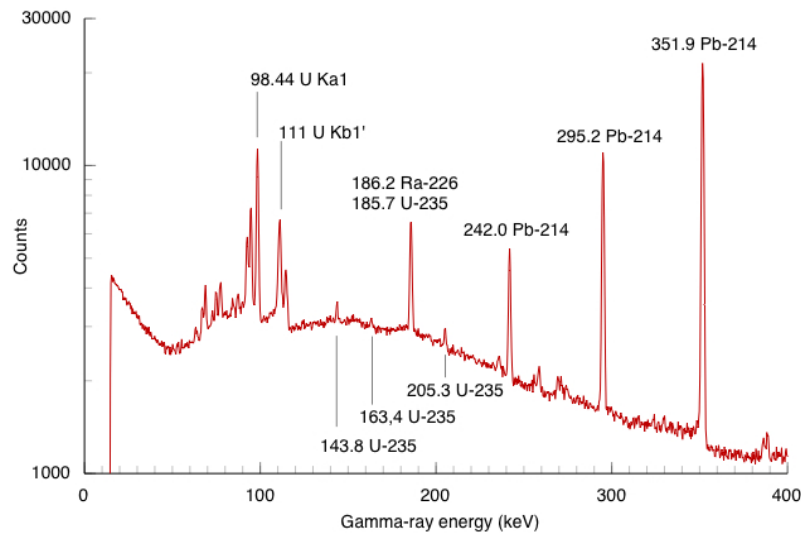


Fig. C-3. An expanded view of the high-resolution gamma-ray spectrum from uranium ore from Fig. C-2 showing the four-peak ^{226}Ra signature. The first of the four peaks is an unresolved doublet with an average energy at around 186-keV, formed by the 186.2-keV peak from ^{226}Ra and the 185.7-keV ^{235}U peak from the Actinium decay series. The other three peaks are from the ^{214}Pb daughters of ^{226}Ra .

The uranium ore spectrum in Fig. C-3 has excellent counting statistics and, to the experienced eye of a gamma-ray spectrometrist, there actually is direct evidence of the presence of ^{235}U . Weak ^{235}U peaks are observable at 143- and 205-keV. Midway between the 143- and 185-keV peaks there is a “nubbin” that is an incipient 163-keV ^{35}U peak. The *RadID* did not find the Poisson signal-to-noise ratios for the 163- and 205-keV peaks to exceed the detection thresholds. The signal-to-noise ratio for the 143 keV peak was just high enough for *RadID* to exceed its signal-to-noise (S/N) threshold of marginality ($4 < S/N \leq 5$) but not to be declared manifest ($S/N > 5$).

More observations about background interference in field measurements

Background radiation is ever present in field spectra and can interfere with the signal of interest from a measured radiation source. If the signal of interest is especially weak, background can even mask the source presence entirely. To mitigate this difficulty, in typical radioanalytical laboratory measurements, samples are prepared by a radiochemist in a standard geometry and counted in a standard geometry in a heavily shielded counting chamber in a laboratory. This dramatically reduces background intensity and diurnal background variation in the chamber and allows for an accurate background measurement when the source is absent.

In contrast, it is extremely difficult to measure a trustworthy background spectrum in the field. Moving or reorienting the detector to obtain a source-free background measurement will frequently produce a measurement that will likely differ significantly, and sometimes even exceeding, the true background at the source position. It is not at all unusual for environmental background to vary significantly over distances of a few meters. As a result, we typically confine our analyses to the foreground spectrum, as generally reflected in this paper.

References

1. Karl E. Nelson, Thomas B. Gosnell, David A. Knapp, *The effect of energy resolution on the extraction of information content from gamma-ray spectra*, Nucl. Instr. Meth. Phys. Research A **659** (2011) 207.
2. Glenn F. Knoll, *Radiation Detection and Measurement*, Third Ed., Wiley, New York 2000, p. 428.
3. Artificial Intelligence, *Rule-based expert systems*, <http://intelligence.worldofcomputing.net/expert-systems-articles/rule-based-expert-systems.html>
4. Adrian A Hopgood, *Intelligent Systems for Engineers and Scientists*, 2nd Ed., CRC Press, pp 1–47, New York, 2001.
5. Edgardo Browne and Richard B. Firestone, with Virginia S. Shirley, Editor, *Table of Radioactive isotopes*, John Wiley and Sons, New York, (1986).
6. Gordon R. Gilmore, *Practical Gamma-ray Spectrometry*, 2nd Ed., Wiley, Hoboken, NJ, 2008, p. 319.
7. Wikipedia, *Uranium-234*, <http://en.wikipedia.org/wiki/Uranium-234>
- ~~8.~~ C. W. Forsburg and L. C. Lewis, *Uses for uranium 233: What should be kept for future needs?*, Oak Ridge National Laboratory Report ORNL-6952, 1999.
- ~~9.~~8. IAEA NAPC Physics Section, WIMS Library Update Project, *Actinides burnup chain*, <http://www-nds.iaea.org/wimsd/achain.htm>
- ~~10.~~9. Wikipedia, *Thorium fuel cycle*, http://en.wikipedia.org/wiki/Thorium_fuel_cycle
- ~~11.~~10. J. Kang and F. N. von Hippel, *U-232 and the Proliferation-Resistance of U-233 in Spent Fuel*, Science & Global Security, **9** pp 1-32.
- ~~12.~~ Charles Barton, *Thorium fuel cycle development in India*, EnergyFromThorium, <http://energyfromthorium.com/2008/04/15/thorium-fuel-cycle-development-in-india/>
11. International Thorium Energy Organisation, Stockholm, Sweden, <http://www.itheo.org>.
- ~~13.~~12. Charles Barton, *Thorium fuel cycle development in India*, EnergyFromThorium, <http://energyfromthorium.com/2008/04/15/thorium-fuel-cycle-development-in-india/>
- ~~14.~~13. Koyel X. Bhattacharyya, *India advances thorium breeding technology*, Stanford energy journal, http://energyclub.stanford.edu/index.php/Journal/India_Advances_Thorium_Breeding_Technology_by_Koyel_Bhattacharyya, Spring 2012.
- ~~15.~~14. Neelima Prasad, Anek Kumar, Umasankari Kannan, Arvind Kumar, P.D. Krishnani, R.K. Sinah, *Study for use of LEU along with Thorium in Advanced Heavy Water Reactor (AHWR) to Enhance Proliferation Resistance Characteristics of Fuel*, IAEA Paper Number: IAEA-CN-184/207.
- ~~16.~~15. Wikipedia, *Uranium-236*, <http://en.wikipedia.org/wiki/Uranium-236>
- ~~17.~~16. Nuclear Engineering International, *GNEP is dead; long live Gen-4*, July 2009, <http://www.neimagazine.com/story.asp?storyCode=2053466>
- ~~18.~~17. Nuclear Engineering International, *DOE releases GNEP plan*, January 2007, <http://www.neimagazine.com/story.asp?storyCode=2041507>
- ~~19.~~18. Ronald J. Ellis, *Prospects of Using Reprocessed Uranium in CANDU Reactors, in the US GNEP Program*, Oak Ridge National Laboratory, 2007, http://www.ornl.gov/sci/scale/pubs/ldoc7152_ans_national_summary_nov2007_rje.pdf

- 20.19. Ahlmad Ibrahim and Kyle Oliver, *Reactor physics analysis of the effects of U-236 poisoning on the use of reprocessed uranium in PWR fuel*, Oak Ridge National Laboratory, 2007, http://kyleoliver.net/work/406_final.pdf
20. Peter Weiss, Science News, Vol. 162 #17, p. 259, 2002, *Neptunium Nukes? Little-studied metal goes critical*, October 2002, <http://www.webcitation.org/6Cw9Vnt0Q>
21. Robert G. Lanier, Catherine F. Hayden, DeLynn Clark, and Winifred E. Parker, *Evaluations of the $^{35}\text{U}/^{238}\text{U}$ isotope ratio through thick-walled containers using the 185.7-keV and 1001.0-keV gamma rays*, Lawrence Livermore National Laboratory report, UCRL-ID-143390 (2001).
22. R. Gunnink, W. D. Ruhter P. Miller, J. Goerten, M. Swinhoe, H. Wagner, J. Verplancke, and S. Abousahl, *MGAU A New Analysis Code for Measuring U-235 Enrichments in Arbitrary samples*, Lawrence Livermore National Laboratory Report, UCRL-JC-114713 Preprint, <http://www.osti.gov/bridge/servlets/purl/10123137-zU1iH9/native/10123137.pdf>, 1994.
23. Thomas B. Gosnell, *Automated calculation of photon source emission from arbitrary mixtures of naturally radioactive heavy nuclides*, Nucl. Instr. Meth. Phys. Research, **A299** (1990) 682.
24. U.S. Department of Energy, New Brunswick Laboratory, http://www.nbl.doe.gov/htm/certified_reference_materials.htm
25. T.S. Zaritskaya, S.M. Zaritskii, A.K. Kruglov, L.V. Matveev, A.P. Rudik, and E.M. Tsenter, *Atomnaya Energiya*, **48** (1980) 67.
26. A.J. Perrung, PNNL-12075, *Predicting ^{232}U Content in Uranium*, Pacific Northwest National Laboratory, Richland, WA, (1998).
27. T. B. Gosnell and B. A. Pohl, *Spectrum synthesis—High-precision, high-accuracy calculation of HPGe pulse-height spectra from thick actinide assemblies*, Lawrence Livermore National Laboratory report, UCRL-JC-120585, 1995.
28. Breismeister, J. F., (editor), Nov. 1993, *MCNP—A General Monte Carlo N-Particle Transport Code*, Version 4A, LA_12625-M, Los Alamos National Laboratory, 3-90.
29. D. J. Mitchell, H. M. Sanger, and K. W. Marlow, *Gamma-ray response functions for scintillation and semiconductor detectors*, Nucl. Instr. and Meth. **A276** (1989) 547.
30. IAEA Safeguards Glossary, 2001 Edition, International Nuclear Verification Series No. 3, International Atomic Energy Agency, p. 23, Vienna, 2002. http://www-pub.iaea.org/MTC/publications/PDF/nvs-3-cd/PDF/NVS3_prn.pdf
31. Health Physics Society, *Answer to Question #1593 Submitted to "Ask the Experts,"* <http://www.hps.org/publicinformation/ate/q1593.html>
32. Alan P. Dickin, *Radiogenic Isotope Geology*, 2nd Ed., Cambridge University Press, Cambridge, UK, 2005, p. 324.
33. U. S. Environmental protection agency, *TENORM in consumer products*, <http://www.epa.gov/radiation/tenorm/consumer.html>
34. Wikipedia, *Abundance of elements in the Earth's crust*, http://en.wikipedia.org/wiki/Abundance_of_elements_in_Earth%27s_crust
35. The University of Sheffield and WebElements Ltd, *Abundance in Earth's crust*, UK, http://www.webelements.com/periodicity/abundance_crust/
36. Jefferson Lab, *It's Elemental—The Periodic Table of the Elements*, <http://education.jlab.org/itselemental/index.html>
37. *Atomic weights of the elements: Review 2000*, Pure Appl. Chem., Vol. 75, No. 6, p. 787, 2003 (*IUPAC Technical Report*), <http://pac.iupac.org/publications/pac/pdf/2003/pdf/7506x0683.pdf>

38. Y. Fujikawa, M. Fukui, M. Sugahara, E. Ikeda and M. Shimada Y. Fujikawa1, M. Fukui, M. Sugahara, E. Ikeda and M. Shimada, *Variation in uranium isotopic ratios $^{234}\text{U}/^{238}\text{U}$ and $^{235}\text{U}/\text{total-U}$ in Japanese soil and water samples —Application to environmental monitoring*, International Radiation Protection Association, <http://www.irpa.net/irpa10/cdrom/00809.pdf>
39. Mineral and locality database, <http://www.mindat.org/>.
40. Mineralogy Database, <http://webmineral.com/cgi-bin/search/search.pl?Realm=All&Match=1&Terms=uranium%20ore&maxhits=10&Rank=1>
41. Wikipedia, *Uranium ore*, http://en.wikipedia.org/wiki/Uranium_ore.
42. *Feature stories: Depleted uranium*, International Atomic Energy Agency, Vienna, http://www.iaea.org/newscenter/features/du/du_qaa.shtml
43. Argonne National Laboratory, *Chemical forms of uranium*, <http://web.ead.anl.gov/uranium/guide/ucompound/forms/index.cfm>
44. Richard L. Meyers, *The 100 most important chemical compounds: a reference guide*, Greenwood Press, Westport, Connecticut, , p. 285 2007.
45. Britannica Online Encyclopedia, *Uraninite (mineral)*, <http://www.britannica.com/EBchecked/topic/619106/uraninite>
46. Argonne National Laboratory, *Uranyl Fluoride*, <http://web.ead.anl.gov/uranium/guide/ucompound/propertiesu/fluoride.cfm>
47. U. S. Nuclear Regulatory Commission, NRC regulations §110.2 *Definitions*, <http://www.nrc.gov/reading-rm/doc-collections/cfr/part110/part110-0002.html>
48. Wikipedia, *Weapons-grade*, <http://en.wikipedia.org/wiki/Weapons-grade>
49. Frank Settle, *Nuclear Chemistry: Uranium Enrichment*, General Chemistry Case Studies, <http://www.chemcases.com/nuclear/nc-07.html>
50. Morten Bremer Maerli, Components of naval nuclear fuel transparency, Norwegian Institute of International Affairs, p. 26, 2002, <http://www.nato.int/acad/fellow/99-01/maerli.pdf>
51. Wikipedia, *Reprocessed uranium*, January 2012, http://en.wikipedia.org/wiki/Reprocessed_uranium
52. World Nuclear Association, *Processing of Used Nuclear Fuel*, May 2012, <http://world-nuclear.org/info/inf69.html>
53. *Radium—Human Health Fact Data Sheet*, Environmental Assessments Division, Argonne National Laboratory, 2005, <http://www.evs.anl.gov/pub/doc/radium.pdf>.
54. bid. ref. 2, p 450.
55. U. S. Department of Energy, *Plutonium: The first 50 years*, DOE/DP-0137, February 1996. <http://www.ornl.gov/ptp/PTP%20Library/library/Subject/Plutonium/plutonium9.pdf>